Concentration of iron ore via reverse cationic flotation of silicates: challenges and solutions

Laurindo de S. Leal Filho

Contents

1. Ore reserves & production

Brazilian Reserves

→ 65% on the Southeast (Minas Gerais)

→ 30% on the North (Carajás)

→ 4% on the West (Urucum)

→ 1% other areas

33 B of tons

Carajás

Minas Gerais

Brazilian Production (2020)

Use	Fe	SiO$_2$
Blast furnace	$\geq 66.5\%$	$\leq 2.5\%$
Direct reduction	$\geq 67.5\%$	$\leq 1\%$

-0.15mm

81.7Mt

Froth flotation

+6.3mm

25.4Mt

Lump 6%

Pellet feed 21%

Sinter feed 73%

281.7Mt

-6.3mm +0.15mm

388.8 Mt
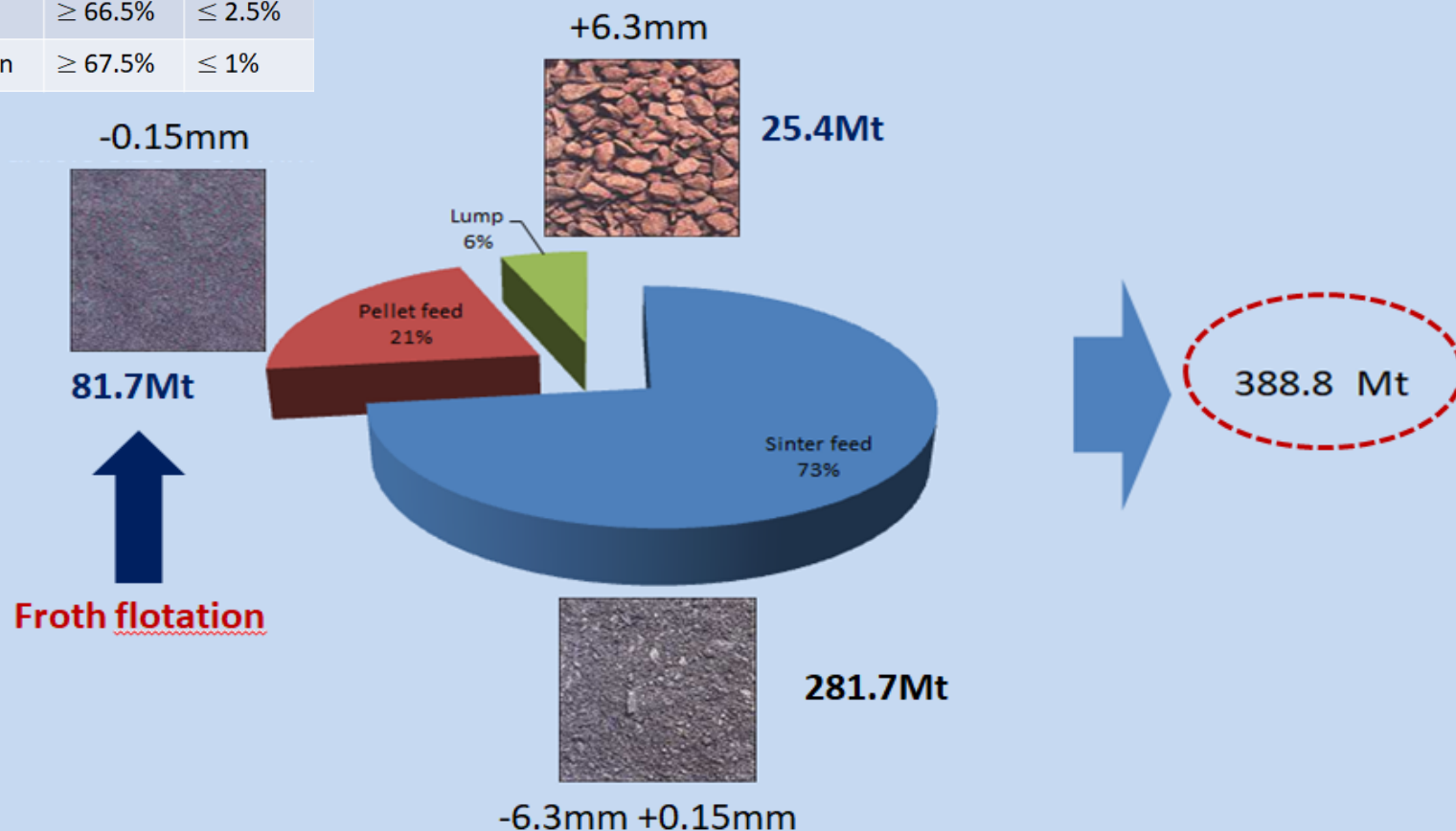
The biggest producers (2020)

Mining Companies

- Vale → 300.5 Mt (2020)
- CSN
- Anglo
- Others

77%
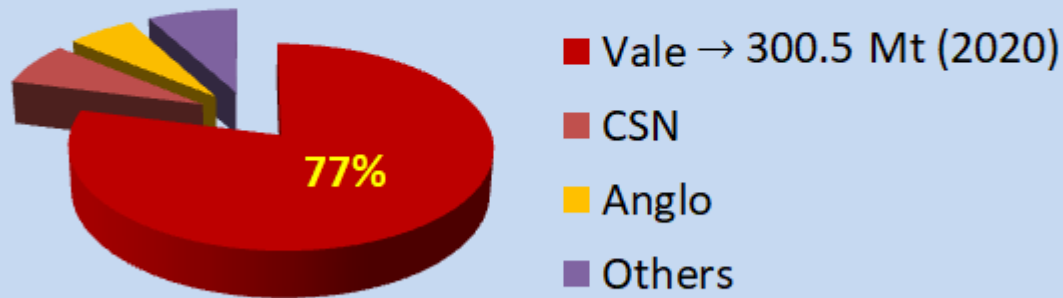
# 2. Typical sorts of ore & beneficiation

Sorts of itabirite

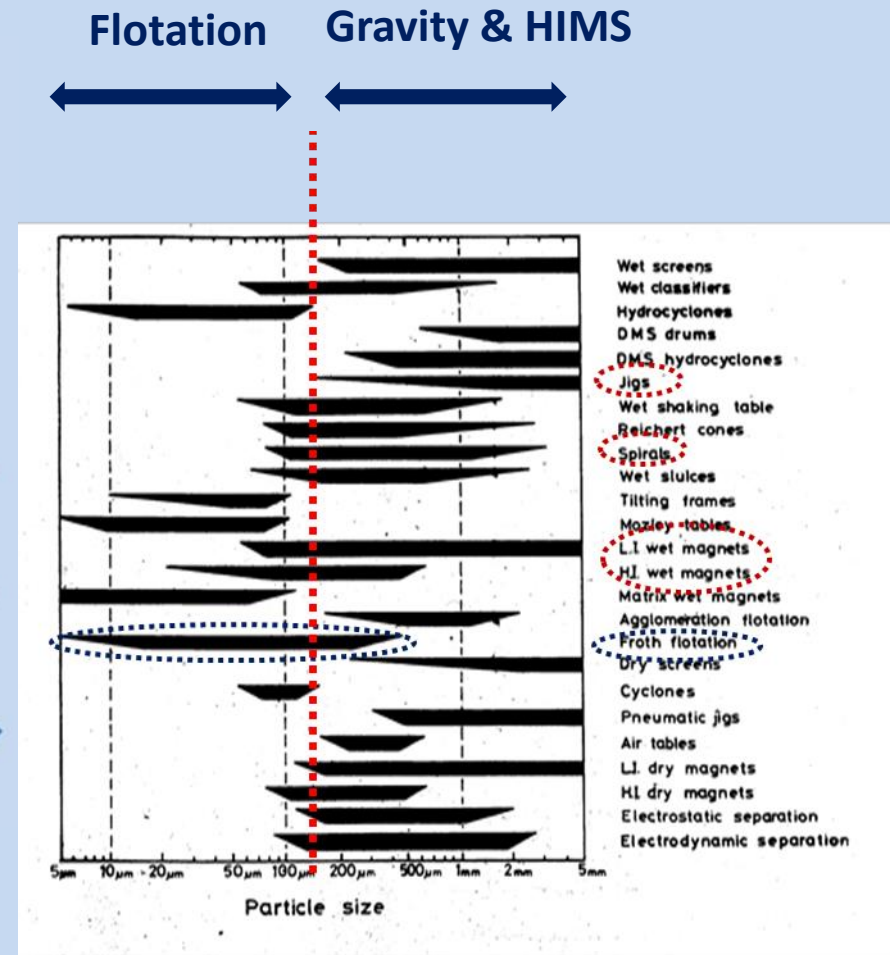| Itabirite (soft and hard)	Main Minerals	Secondary Minerals
Standard Itabirites (50% < Fe < 60%)	Fe-Oxides (*) Quartz	Phylosilicates Dolomite Mn-Oxides
Dolomitic Itabirites (50% < Fe < 60%)	Fe-Oxides (*) Dolomite	Quartz Phylosilicates Mn-Oxides
Amphibolitic Itabirites (50% < Fe < 60%)	Fe-Oxides (*) Amphibole	Quartz Dolomite
High grade Fe > 65%	Hematite	Quartz, magnetite, pyrophylite
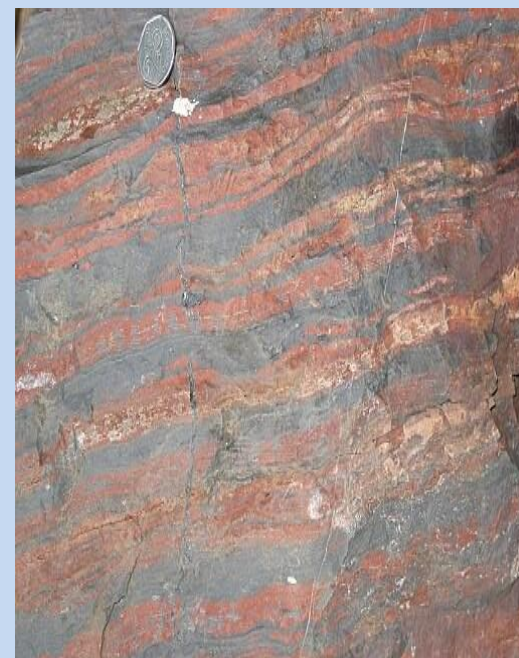
(*) Hematite, magnetite, martite, goethite.

Generic flowchart (hard and soft itabirite)
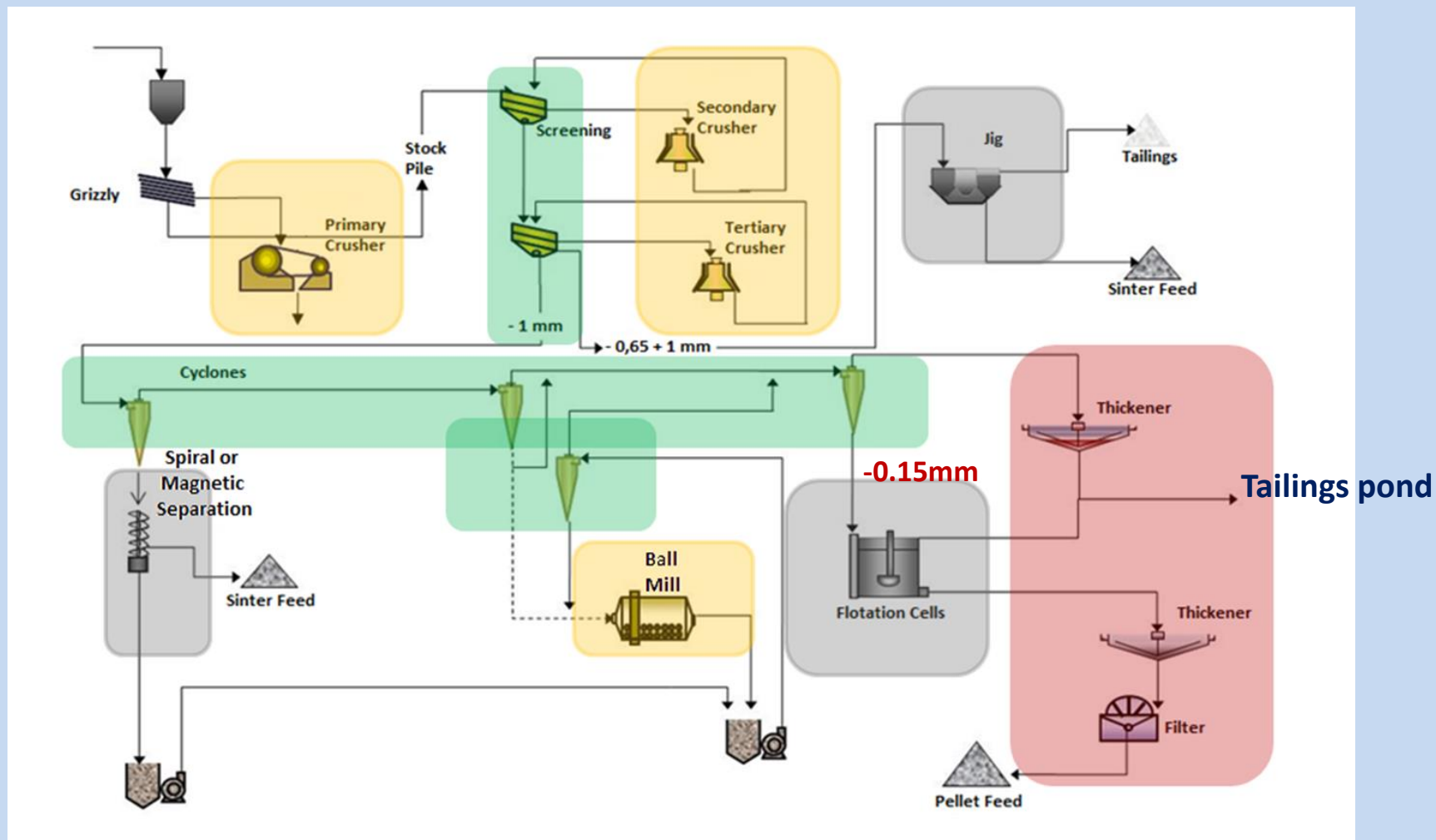
Evolution of the beneficiation over time
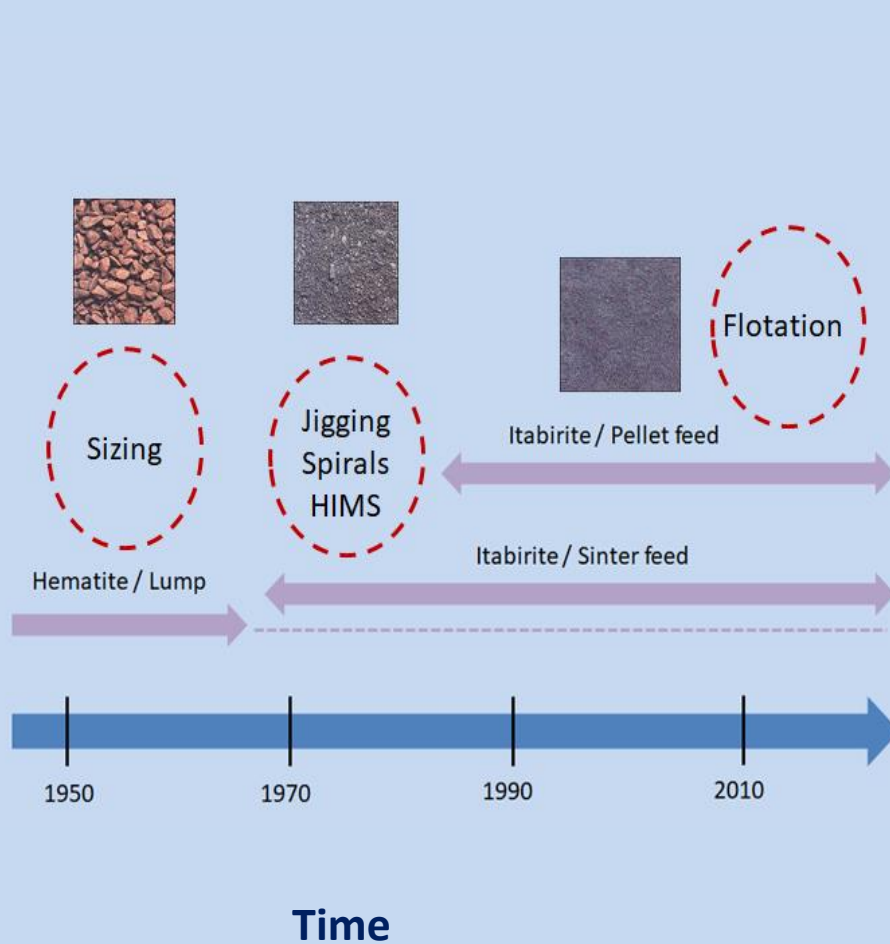
Industrial flowsheet adopted by Samarco to yield pellet feed

ROM

$D_{90}=50\mu m$

$D_{90}=170\mu m$

AMIDO

MINERODUTO

Pipeline

Primary grinding & sizing

Crushing & Screening

Desliming & starch conditioning

Flotation of fine particles
X
Flotation of coarse particles

Regrinding & flotation (-74µm)
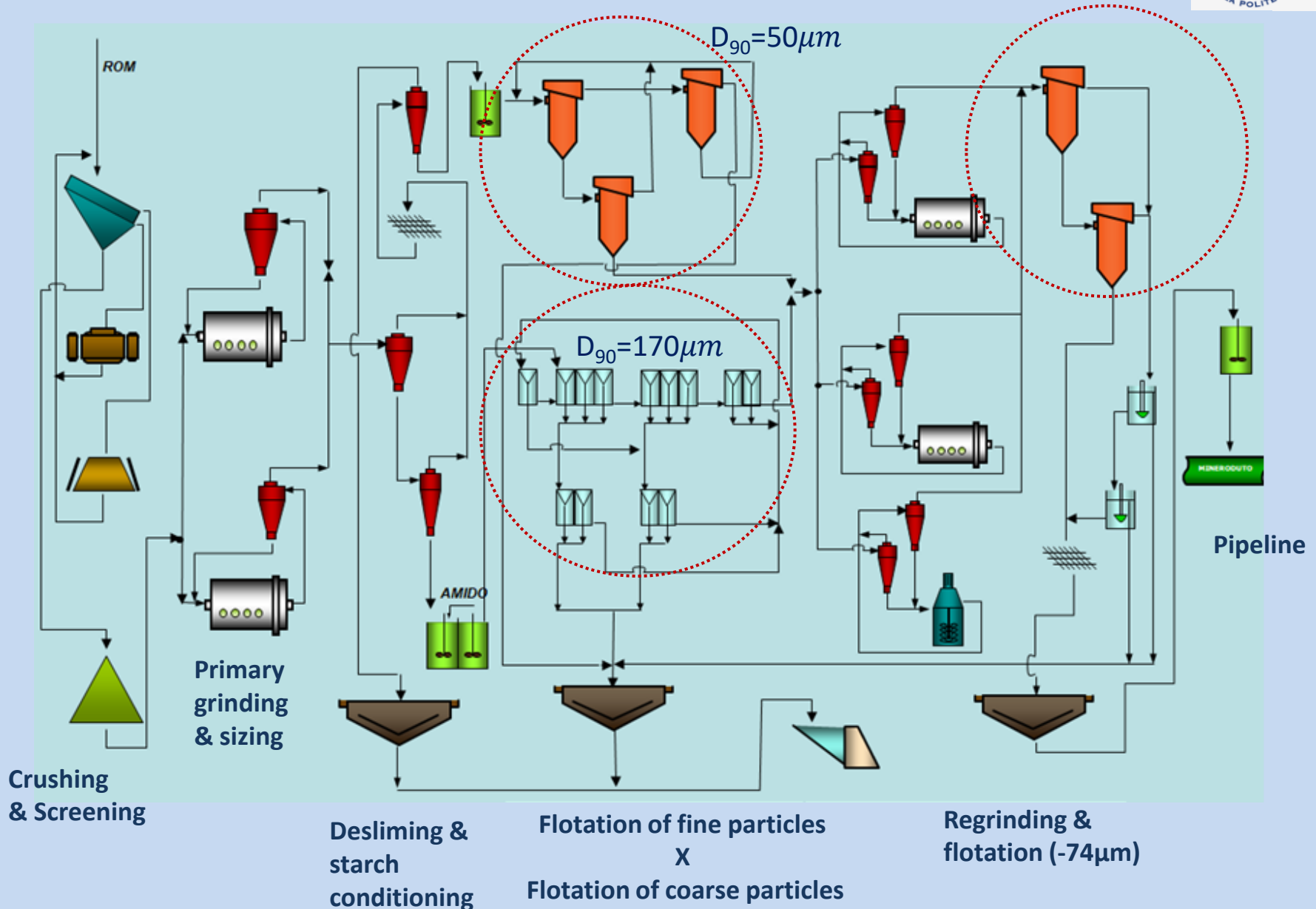
3. Reverse cationic flotation of quartz

3.1 Settled experience

Standard concentration
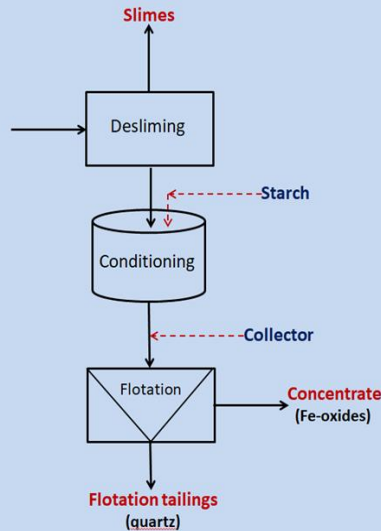
→ Corn starch: depressant for Fe-oxides
400-600 g/t – conditioning time > 5 min.
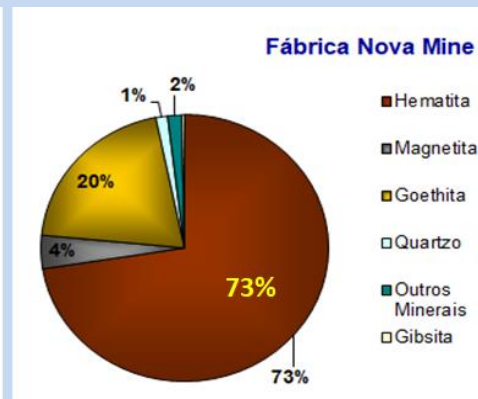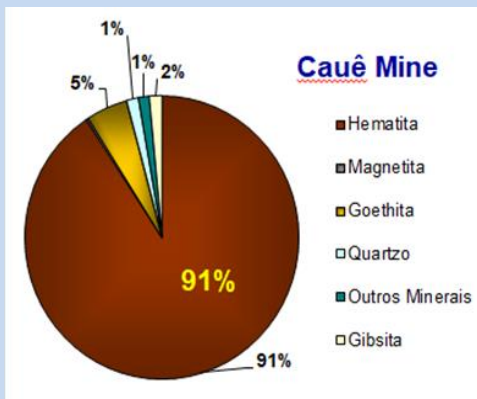
→ Alkyl ether amine (*): collector for quartz
200 g/ton(**) – short conditioning time

(*) Neutralized with CH_3COOH up to 50%
(**) grams per ton of SiO_2

→ Flotation is carried out in basic medium
 (9.0 < **pH** < 10.6) under 40-50% of solids (weight basis)
or 18-25% solids (volume basis)
→ Rougher, cleaner and scavenger.

The quality of the iron concentrate varies according to the mine.

Influence of flotation pH and amine species
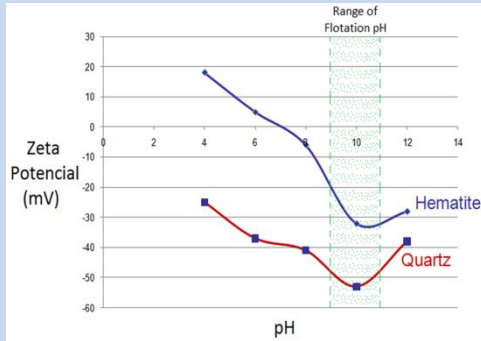
- In the range of flotation pH (9.0-10.6) particles of quartz and hematite are negatively charged.
- To promote the selectivity, it is mandatory to use starch to depress Fe-bearing oxides.

The highest recovery occurs at 10.0<pH<10.6 $\leftrightarrow$ $[RNH_3^+] = [RNH_2]$

Model proposed by Gaudin-Fuerstenau (1976)
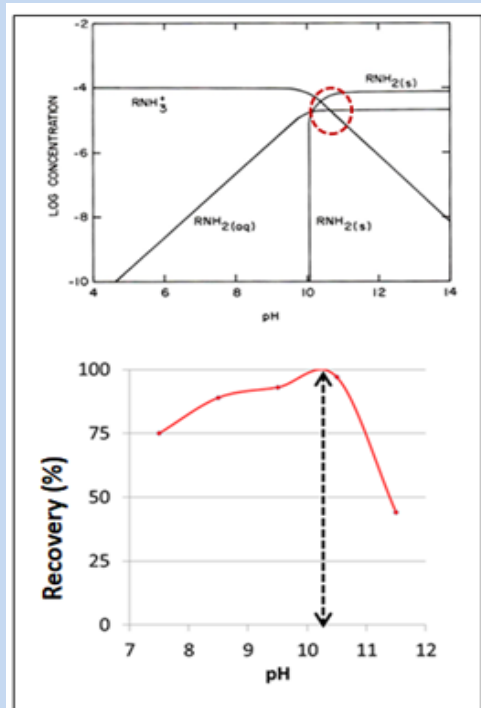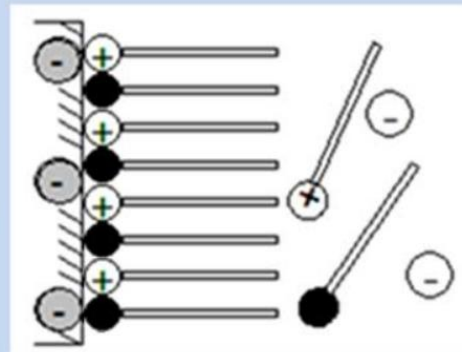
Quartz   Solution

- Contra ion
- Íon determinador de potêncial
+ Coletor catiónico
● Coletor não iônico

As pH>>10.5
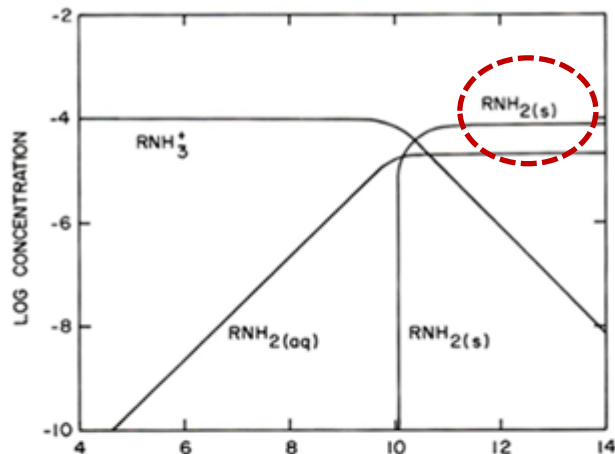
As pH$\gg$ 10.5 → Precipitation of species $NH_2(s)$

The recovery of quartz decreases steadily
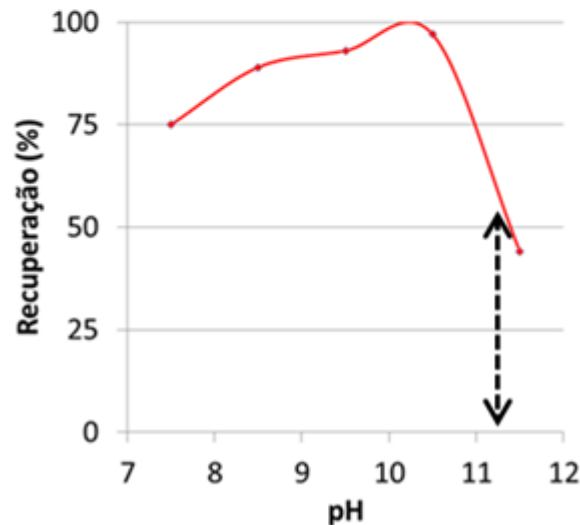
Once in the past, a truck containing NaOH inadvertently poured its load in the tank of amine (instead of in the tank of starch) and then it occurred the formation of a gel that firmly adhered to the walls. It took many days to clean the tank.

Fe-bearing oxides are depressed by corn starch

AMIDO - 60 %
CASCA - 6,5 %
GLÚTEN - 10%
GERME - 8,5%
ÁGUA - 15%
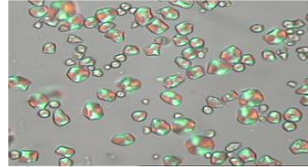
Corn
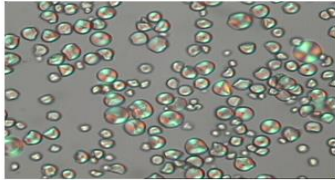
Manioc
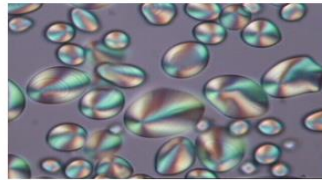
Potato

Sources	Amylose %	Amylopectin %
Corn	27	73
Corn (Waxy®)	< 6	> 94
Manioc	17	83
Potato	20	80
Rice	17	83
Wheat	25	75

AMYLOSE
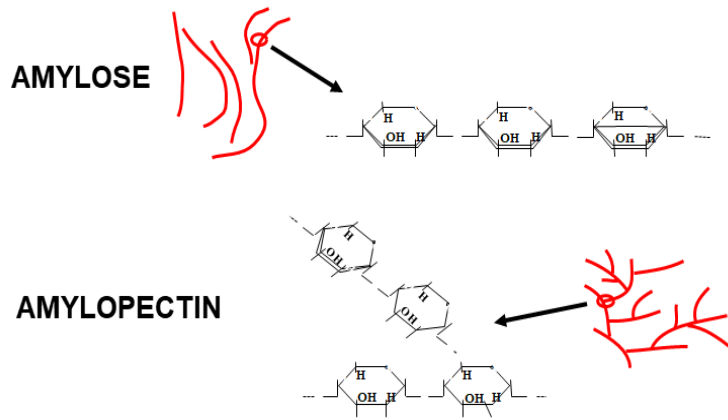
AMYLOPECTIN

Research conducted in the 60's by Iwasaki and co-workers (USA) provides experimental evidence that amylopectin is a better depressant for Fe-bearing minerals than amylose.

Peres and co-workers → Corn gritz (yellow flour) can replace purified starch (white flour) without jeopardizing flotation performance. Gritz is 3 times cheaper than purified starch.

Preparation of starch: gelatinization

Cooking
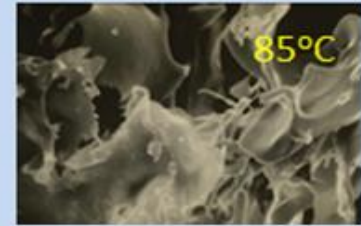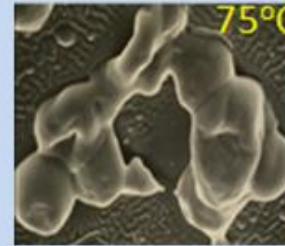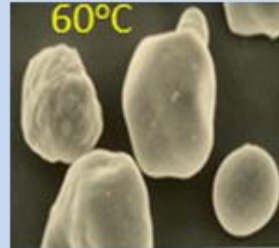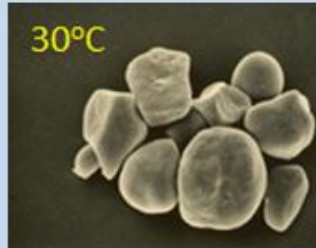
Source: Ingredion®

Leaching
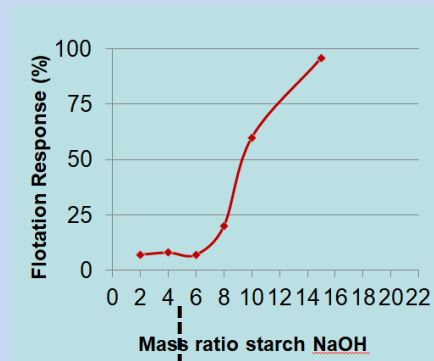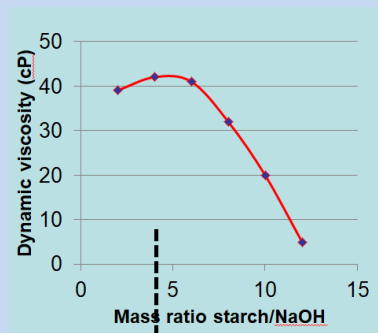
Best ratio starch/NaOH = 4.5-5.0

Starch =500g/t
Flotigam®EDA = 300 g/t
Ore from Conceição Mine

3. Reverse cationic flotation of quartz

3.2 Influence of water quality

Influence of water quality
(the role played by hydrolyzed species)

Water quality severely impacts the reverse cationic flotation of quartz, as hydrolyzed species $MgOH^+$ and $MnOH^+$ are able to adsorb onto quartz/water interface reducing the magnitude of zeta potential and even reversing its sign.

$MgOH^+ \rightarrow 10 < pH < 11$

$MnOH^+ \rightarrow 9.5 < pH < 10.5$

Influence of water quality
(the role played by Ca^{2+})

After conditioning
with dolomitic
itabirite

Regular water

Floatabilitiy of quartz (%)

-log[Ca]
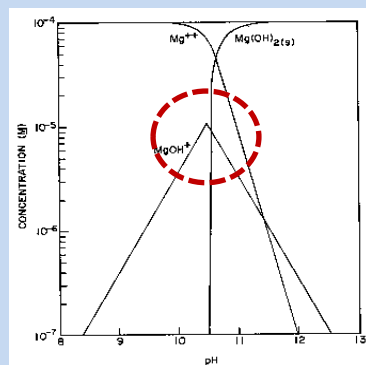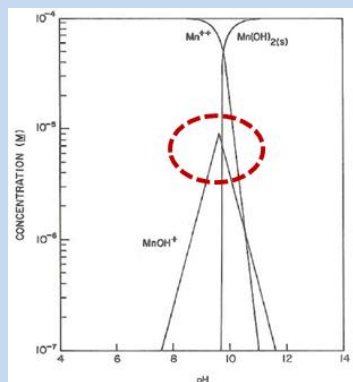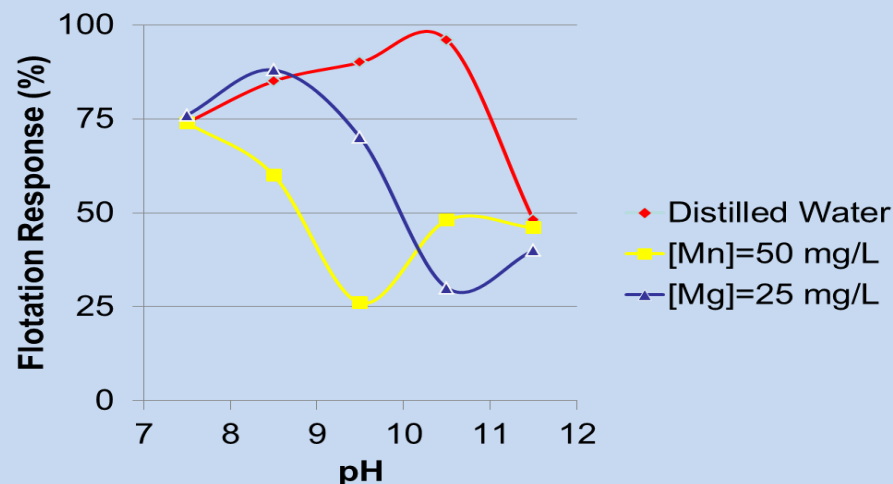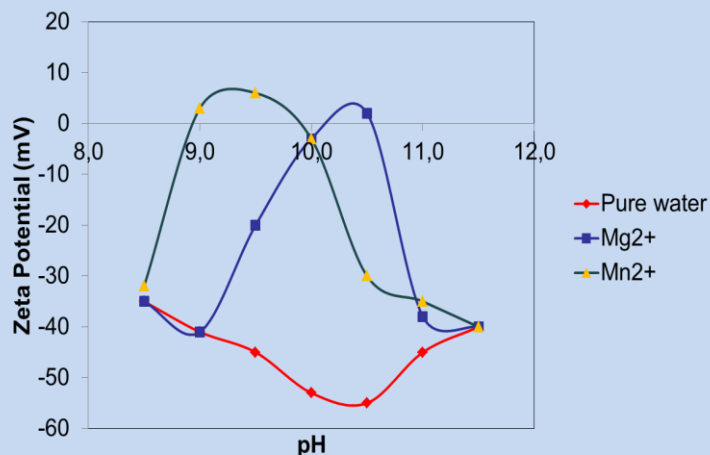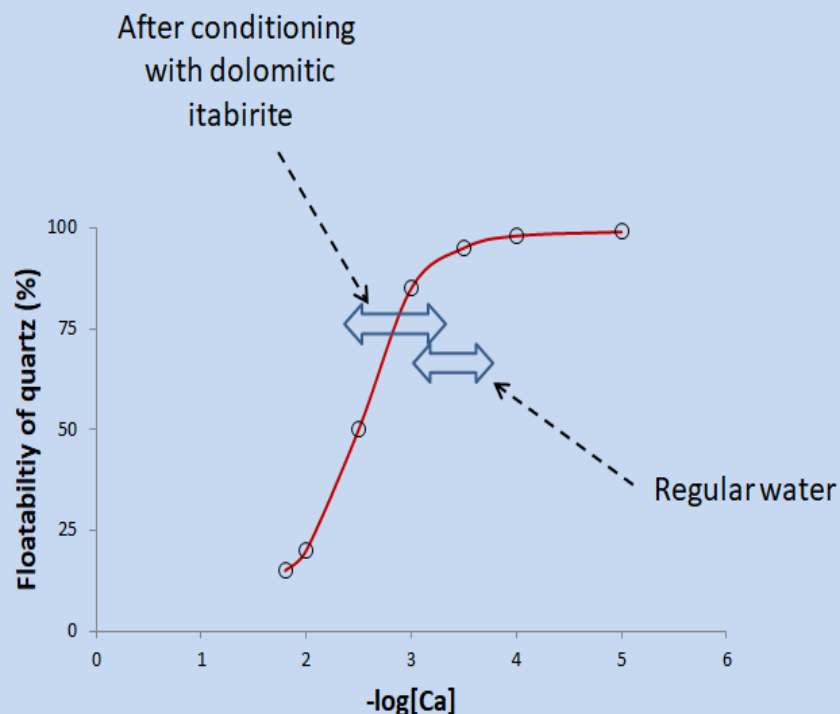
Flotigam®EDA = 15mg/L
Absence of starch

→ Cations Ca^{2+} are able to compress the electrical double-layer of quartz/solution interface eventually reducing the magnitude of zeta potential of quartz particles;

→ Cations Ca^{2+} may compete with cationic collector species $R-O-R-NH_3^+$ for anionic sites at quartz/water interface;

→ This problem commonly occurs when cationic reverse flotation of quartz is carried out with itabirite which is rich in dolomite (5% of dolomite in the flotation feed is sufficient to impact the flotation of quartz particles).

3. Reverse cationic flotation of quartz

3.3 Refractory ores

Refractory ores

Itabirite (soft and hard)	Main Minerals	Secondary Minerals
Standard Itabirites (50% < Fe < 60%)	Fe-Oxides (*) Quartz	Phylosilicates Dolomite Mn-Oxides
Dolomitic Itabirites (50% < Fe < 60%)	Fe-Oxides (*) Dolomite	Quartz Phylosilicates Mn-Oxides
Amphibolitic Itabirites (50% < Fe < 60%)	Fe-Oxides (*) Amphibols	Quartz Dolomite

Very fine particles of Mn-oxides or clays that exchange Mn^{2+} jeopardize the quality of flotation water;

Hard itabirite demands enhanced grinding circuits;

The presence of dolomite increases the concentration of Ca^{2+} and $MgOH^+$ in solution;

The Isoelectric Point (IEP) of amphiboles occurs at 3<pH<4, whereas IEP of quartz happens at pH≈2.

The surface of the particles of amphiboles are less negatively charged than quartz particles and eventually show a poor flotation performance.

At pH=10.5 (KCl 1×10^{-3}M):

→ Zeta potential of quartz = **-54mV**

→ Zeta potential of hornblenda = **-32mV**

Stronger collectors as diamines are required?

3. Reverse cationic flotation of quartz

3.4 The behavior of coarse particles

Particle size distribution and chemical composition of a typical hematite concentrate

Fração granulométrica					Teor %				
Peneiras		% Retida simples	% Acumulada	% Passante	Fe	SiO$_2$	Al$_2$O$_3$	P	PPC
Tyler	μm								
35	420	0,62	0,62	99,38	47,77	25,56	1,11	0,058	4,86
48	297	1,98	2,60	97,40	52,72	18,75	0,71	0,062	4,98
65	210	2,86	5,46	94,54	57,38	12,01	0,95	0,064	4,81
100	149	10,45	15,91	84,09	61,23	7,69	0,40	0,056	4,09
150	105	7,40	23,31	76,69	64,05	4,56	0,33	0,048	3,36
200	74	15,81	39,12	60,88	65,90	2,57	0,30	0,043	2,81
270	53	16,81	55,93	44,07	66,90	1,23	0,24	0,035	2,28
325	44	6,71	62,64	37,36	67,62	0,92	0,22	0,031	1,91
400	37	6,41	69,05	30,95	67,98	0,77	0,19	0,030	1,75
-400	-37	30,95	100,00	-	67,82	0,63	0,26	0,033	1,89
Cabeça calculada					65,67	2,93	0,31	0,040	2,60
Cabeça analisada					65,80	3,08	0,30	0,039	2,66

Use	Fe	SiO$_2$
Blast furnace	≥ 66.5%	≤ 2.5%
Direct reduction	≥ 67.5%	≤ 1%

Mass Recovery = 74-78%   Fe Recovery = 82-88%

Coarse quartz particles **(+0.15mm)** show **poor** flotation response

Why coarse particles exhibit a poor flotation performance?
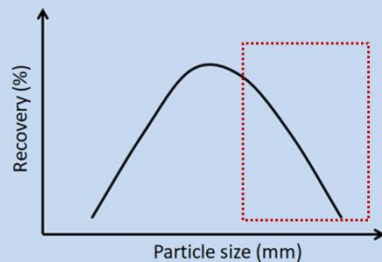
$$E_K = E_c \cdot E_a \cdot E_p$$

E_K = Efficiency of particle collection by a bubble;

E_C = Efficiency of particle/bubble collision;

E_a = Efficiency of particle/bubble adhesion;

E_p = Efficiency of the preservation of the particle/bubble aggregate;

Kinetic constant = $k = \dfrac{1}{4} S_b E_K$ (1st order model)

S_b = Surface bubble flux [s^{-1}]
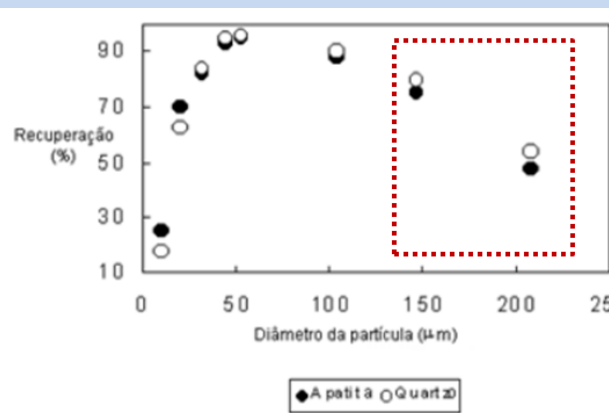
The phenomenon of particle/bubble detachment is caused by turbulence that exists inside flotation equipment.

Detachment promotes a decrease in the value of E_P, delaying flotation kinetics and decreasing the recovery.

When the content of SiO_2 in the hematite concentrate is higher than 2.5%, mill men are **"mentally programmed"** to increase **the collector dosage**, aiming at increasing the flotation of quartz.

Slimes

Desliming

Starch

Conditioning

Collector

Flotation

Concentrate
(Fe-oxides)

Flotation tailings
(quartz)
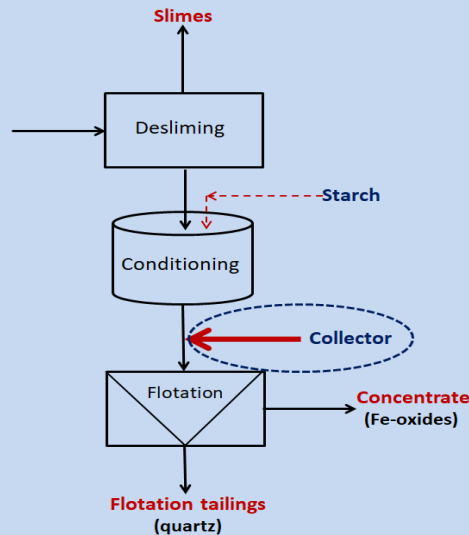
However... In many occasions, the increase in the collector dosage decreases the recovery of quartz in the froth even more!

High content of SiO_2 in the concentrate is generally due to the presence of coarse particles of quartz that float very badly.

Attachment
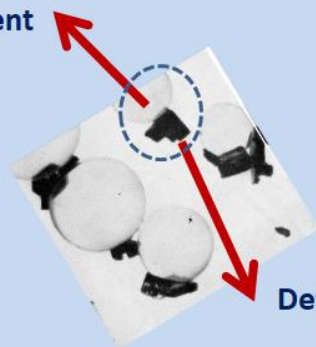
Detachment

Coarse particles are able to collide pretty well with bubbles, but **fail to remain attached** to them due to the existing **turbulence** in the flotation cells.

The equilibrium could be idealized as an arm wrestling...

$$F_{Cap} = \pi \, d_p \sin\omega \, \sin(\omega + \theta)$$

d_p = Particle diameter;
ω = Central angle of the particle
θ = Contact angle
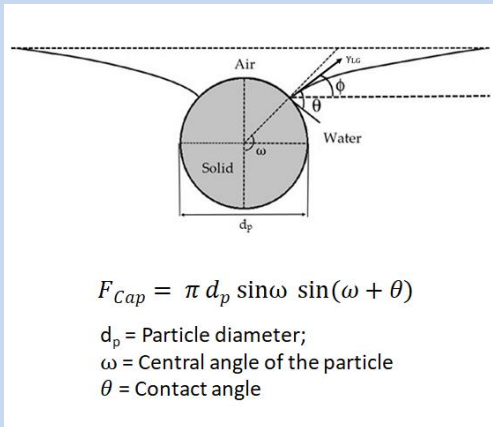
Attachment ⟷ **Detachment**

Inertial forces
- Tensile stresses
- Compressive stresses
- **Shear** stresses

+ **Gravity forces**
- Weight

Mine/Mill	Collector Flotigam®EDA	Depressant Corn starch	Slurry	
			% solids (w/w)	Surface tension
Brucutu-MG (rougher stage)	75mg/L	215mg/L	55%	(**51.2±0.5**) mN/m

The more collector is added to the flotation slurry, the lower is the value of the surface tension (γ) of flotation solution and eventually the value of contact angle (θ).
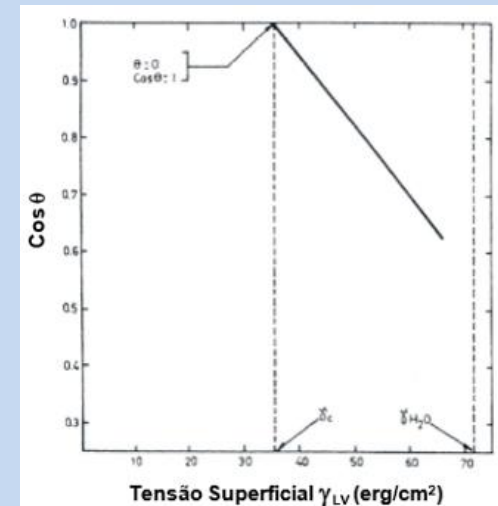
Source: Oscan, 1992

Critical surface tension of wettability of quartz after collector adsorption

Resin-embedded chunk of quartz

Contact Goniometer (captive bubble method)
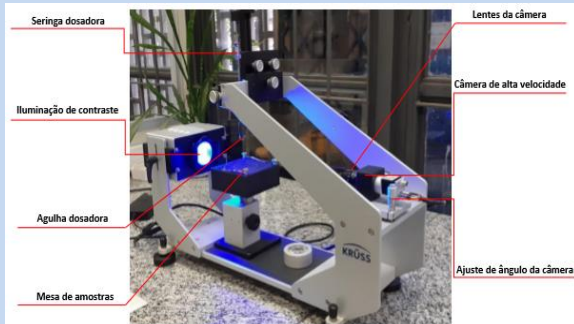
Tensiometer (Wilhelmy plate method)
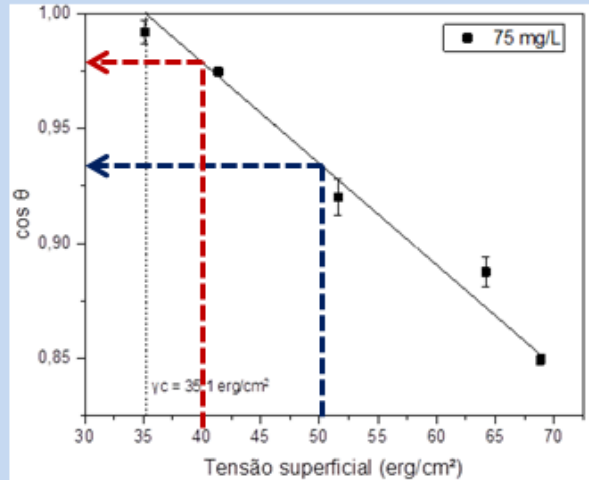
Collector dosage ↑

$\gamma_{L/G}$↓

$\cos\theta$ ↑ θ↓

Quartz floatability ↓

Surface Tension	Contact angle
51 mN/M	24º
40 mN/m	20º
35 mN/m	0º

Critical surface tension of wettability of quartz = 35.1 mN/m

Minimum contact angle of quartz to promote the flotation of quartz particles

----

Coarse particles →

147µm
104µm
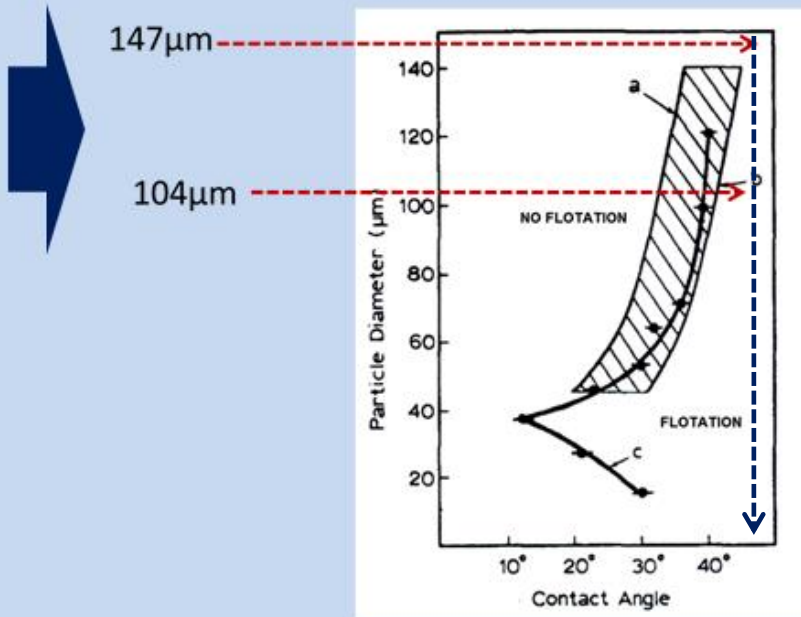
Source: Ralston et al., 1988

Demanded values of θ
to float quartz coarse particles

$$147\mu m \leftrightarrow \theta \geq 38^o$$

$$104\mu m \leftrightarrow \theta \geq 45^o$$

Minimum contact angle of quartz to promote the flotation of quartz particles

----
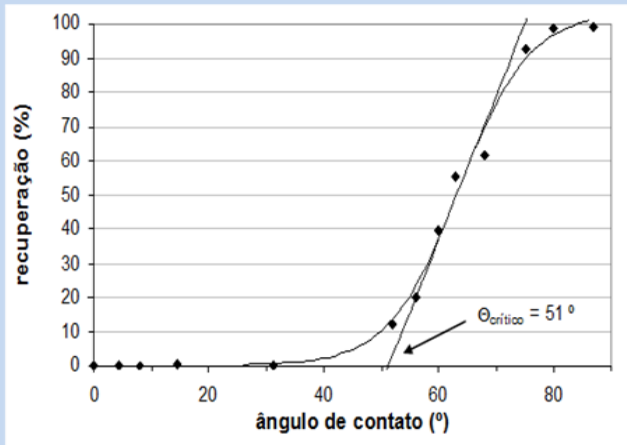
Source: Gontijo, 2010

Surface Tension	Contact angle
51 mN/M	24°
40 mN/m	20°
35 mN/m	0°

Critical value of contact angle for coarse particles of quartz to float = $\theta_{Critical}$

$$\theta_{Critical} = 51°$$

Values of θ (20°-24°) typically found in the industrial flotation circuit ($\gamma_{L/G} = 51$mN/m) of Brucutu are very much lower than the critical value of θ for coarse particles to float ($\theta_{Critical} = 51°$).

Why flotation columns have bad reputation to concentrate coarse particles of quartz and apatite?
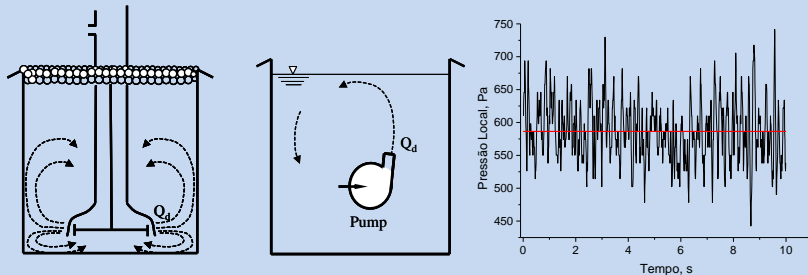
Impeller´s Reynolds number > 10^5

$$R = R_{max} \frac{kt}{(1 + kt)}$$ Mixing reactors
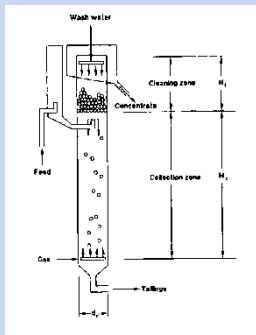
How particles detach from bubbles in columns?

$$R = R_{max} (1 - e^{-kt})$$ Plug flow reactor

Bubble dynamics in columns

Only water

Water + surfactants
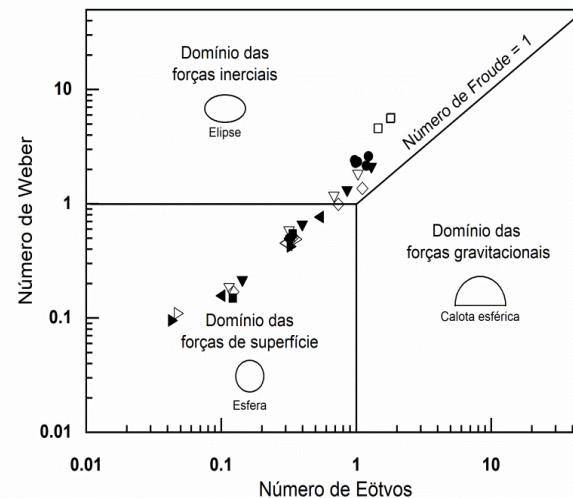
$$Weber\ Number = \frac{d_b^2 \rho g}{\gamma_{LG}} = \frac{Inertial\ forces}{Surface\ forces}$$

$$E\ddot{o}tvos\ Number = \frac{v_b^2 \rho d_b}{\gamma} = \frac{Gravity\ forces}{Surface\ forces}$$

$$Froude\ Number = \frac{Inertial\ forces}{Gravity\ forces} = \frac{v_b^2}{g d_b}$$

$v_b \uparrow$

$d_b \uparrow$

Weber number >1

Weber number < 1

d_b = bubble diameter
v_b = bubble velocity
ρ = fluid specific gravity
γ = surface tension of solution
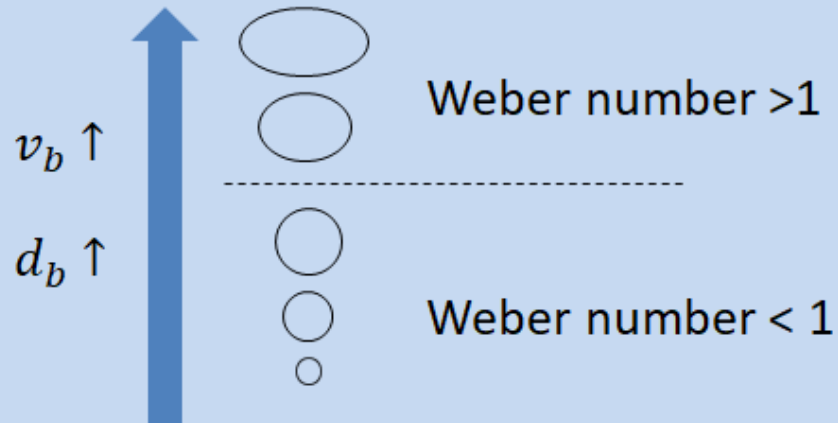
When a bubble rises in a water column, there is an increase in its diameter due to a continuous pressure relief
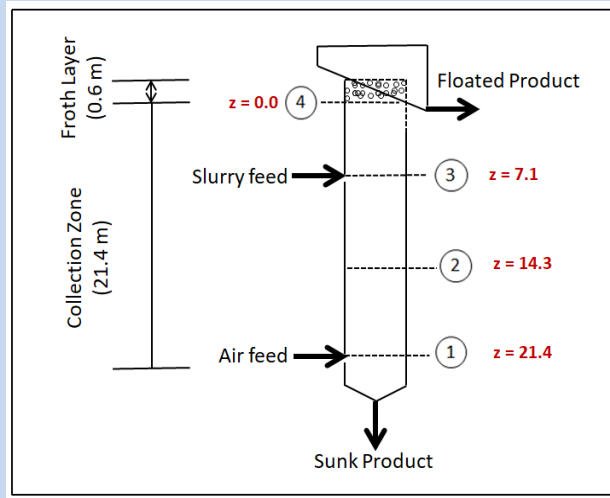
A hypothetical flotation column located at 730m above the sea level ($P_{atm} \approx$ 93 kPa)

Iron ore slurry containing 50% of solids (w/w), gas holdup of 10% and specific gravity of 1,430kg/m^3 (aerated pulp).

Hydrostatic pressure = P_{hyd} = 1,430 x 9,81 x z

Overall static pressure = P_e= P_{hyd} + P_{atm}

$$P_e = P_{hyd} + P_{atm}$$

$$\Delta P = Pi - Pe = \frac{4\gamma}{d_b}$$

Marks	Distance (X) from the baseline along the vertical axis (m)	Height (h) of the slurry column above any level (m)	Static load (kPa)		Overall static pressure (*)
			Atmospheric pressure	Hydrostatic pressure	
Level-1	0.0	21,4	93	308	401
Level-2	7.1	14.3	93	200	293
Level-3	14.3	7.1	93	100	193
Level-4	21.4	0.0	93	0	93

(*) External pressure exerted by the slurry over the bubble (P_e)
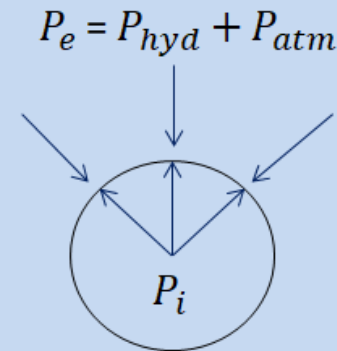
The influence of the bubble external pressure on bubble equivalent diameter and contact angle
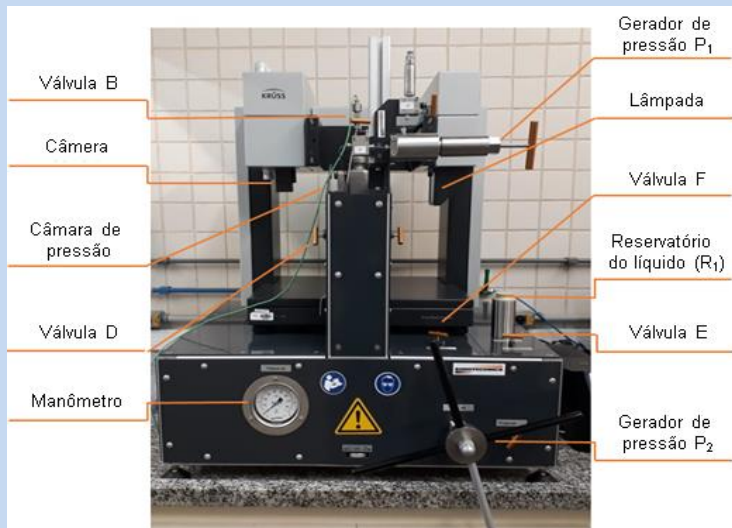
On the top, $d_b \uparrow$ and $\theta \downarrow$

On the top, We>1 → inertial forces dominate over surface forces;

→ Detachment is more likely to happen on the top than on the buttom of the column.
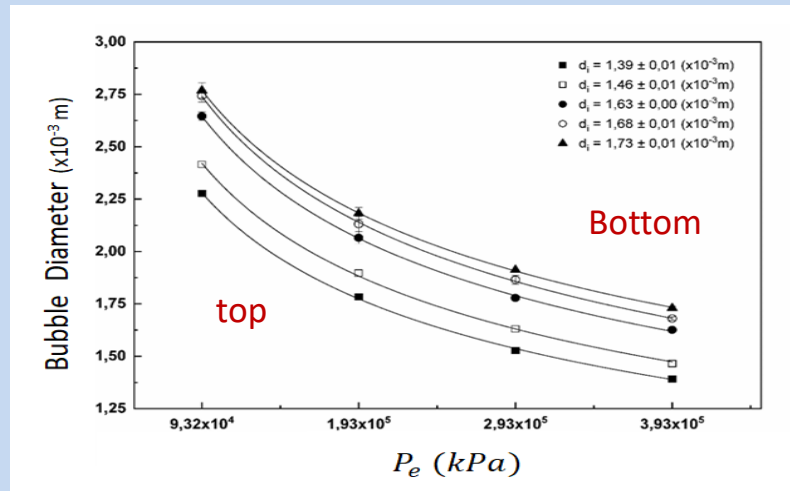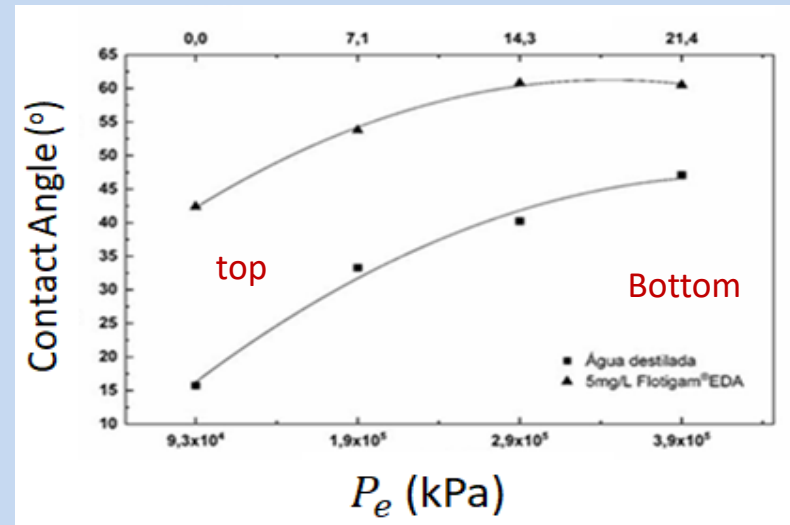
Flotation of coarse particles: columns x mechanical cells

$$R = R_{max} \frac{kt}{(1 + kt)}$$

Mixing reactors
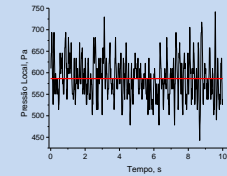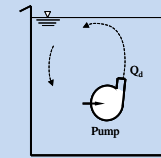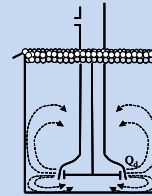
$$R = R_{max} (1 - e^{-kt})$$

Plug flow reactor
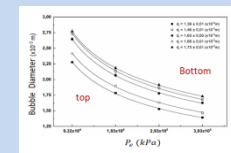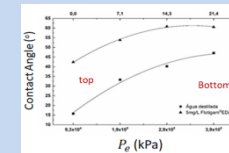
Harsh hydrodynamic conditions either in mechanical cells or in columns contribute to particles detach from bubbles. However…

Mechanical cells (mixing reactors) offer more opportunities for coarse particles to float, whereas columns (plug flow reactor) offer just a single opportunity for particles to float.

3. Reverse cationic flotation of quartz

3.5 Depression of Fe-bearing oxides

Samples of Fe-bearing oxides used in exploratory studies

Particle size	PEAN	PEFA	PXCE	PEFN	PEAL	PXFN	PFGOE	PFMQ	PFMAG
+ 0,150	2,1	3,5	6,6	1,5	3,1	8,9	9,8	7,0	7,1
+ 0,037	83,3	29,4	71,1	60,6	54,8	62,0	78,2	81,8	86,6
- 0,037	14,6	67,1	22,3	37,9	42,1	29,1	12,0	11,2	6,3
TOTAL	100,0	100,0	100,0	100,0	100,0	100,0	100,0	100,0	100,0

Mines	Fe grade (%)	Platy-shaped hematite	Granular Hematite	Martite	Magnetite	Goethite
PEAN	69.1	24.1	67.2	1.8	0.5	3.4
PEFA	66.6	20.7	66.8	6.3	0.4	4.4
PXCE	68.9	23.7	74.0	0.0	0.1	0.4
PEFN	66.9	19.0	60.0	9.3	1.3	9.8
PEAL	68.1	20.5	39.9	25.0	2.3	11.4
PXFN	65.1	11.8	59.7	15.0	4.3	7.6
PFGOE	68.7	0.3	3.3	72.3	1.4	18.8
PFMQ	68.2	0.4	3.4	71.3	4.8	19.2
PFMAG	67.4	0.5	5.0	29,2	58.1	6.6

Floatability of samples containing Fe-bearing oxides in the absence of starch versus concentration of Flotigam®EDA (pH10.5)

Selected results

| Samples | Experimental conditions | | | Floatability (F) |
	pH (*)	Flotigam®EDA concentration (**)	Flotation time (***)	
PXCE	7,66	462 g/t	2' 16"	87%
PEAL	8,52	231 g/t	2' 03"	69%
PFGOE	8,20	462 g/t	1' 47"	37%
PFMQ	8,40	462 g/t	2' 02"	36%
PFMAG	8,83	462 g/t	0' 57"	12%
PEFN	7,72	231 g/t	1' 43"	76%
PXFN	7,54	231 g/t	2' 08"	59%
PEFA	7,68	231 g/t	2' 50"	91%
PEAN	7,60	462 g/t	2' 48"	98%

(*) Natural pH of the pulp, before dosing reagents;
(**) Dosage necessary to obtain maximum floatability;
(***) Flotation time required to obtain the exhaustion of mineralized froth.

Floatability of hematite with Flotigam®EDA in the absence of starch at pH10.5

→ Highest floatabilities (>90%) → samples containing hematite >86%

→ Lowest floatabilities (<37%) → samples that contain magnetite >57% or martite >70%.

Samples	Experimental conditions			Floatability (F)
	pH (*)	Flotigam®EDA concentration (**)	Flotation time (***)	
PXCE	7,66	462 g/t	2' 16"	87%
PEAL	8,52	231 g/t	2' 03"	69%
PFGOE	8,20	462 g/t	1' 47"	37%
PFMQ	8,40	462 g/t	2' 02"	36%
PFMAG	8,83	462 g/t	0' 57"	12%
PEFN	7,72	231 g/t	1' 43"	76%
PXFN	7,54	231 g/t	2' 08"	59%
PEFA	7,68	231 g/t	2' 50"	91%
PEAN	7,60	462 g/t	2' 48"	98%

(*) Natural pH of the pulp, before dosing reagents;
(**) Dosage necessary to obtain maximum floatability;
(***) Flotation time required to obtain the exhaustion of mineralized froth.

98% Hematite

60% Hematite+25% Martite+11% goethite

72% Martite + 19%goethite + 4% hematite

72% Martite + 19% goethite + 5%magnetite +6% hematite.

58% Magnetite +29% martite + 7%goethite +6% hematite.

72% Hematite + 15% Martite + 8% goethite+ 4% magnetite

88% Hematite + 6% Martite + 4% goethite

91% Hematite + 3% goethite + 2% martite

Floatability of hematite with Flotigam®EDA in the absence of starch versus zeta potential (pH10.5)
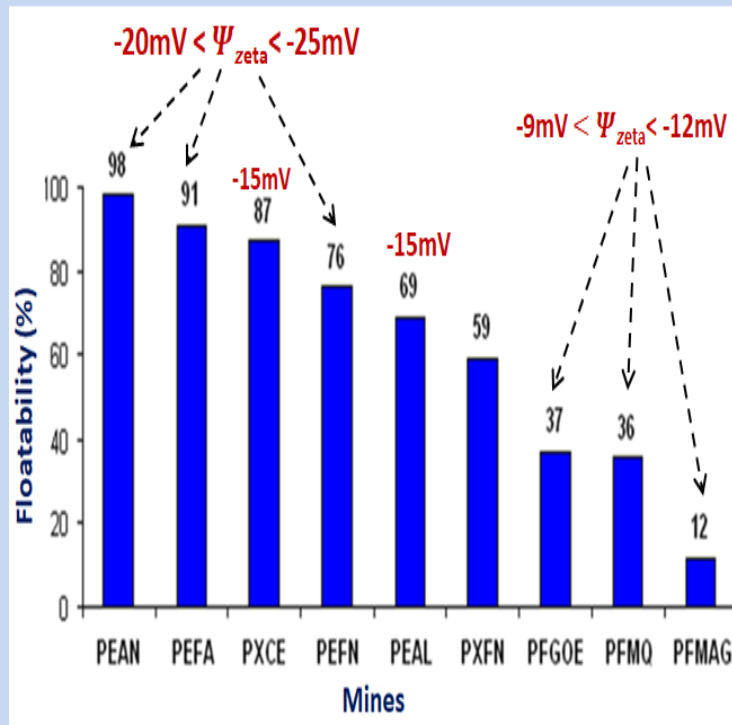
The most negative values of zeta potential can be associated to the highest floatabilities (except PXCE)

The lowest floatabilities (>37%) were achieved with Fe-oxides that exhibit the least negative values of zeta potential: $\leq$ -12mV.

The use of depressant (starch) is a must for 8 out of 9 mines.

Starch did not depress the sample which is rich in magnetite (PFMAG).

Depression of Fe-bearing oxides by corn starch (Flotigam®EDA= 231-462g/t, pH10.5)
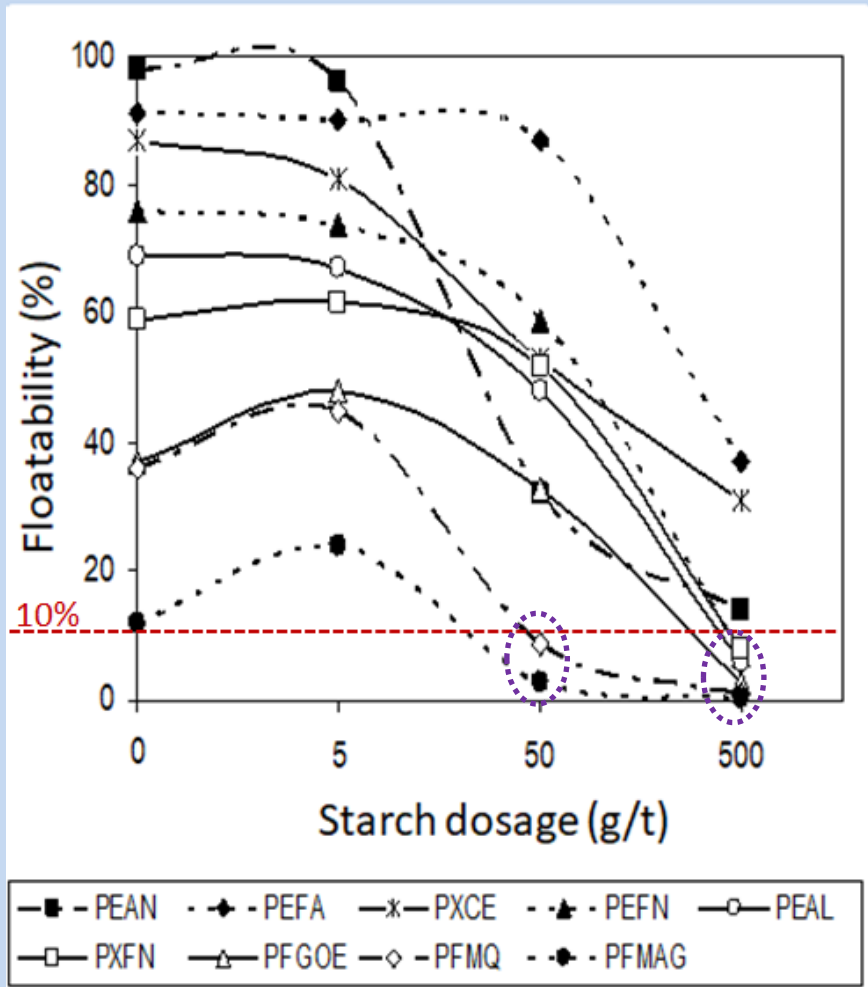
50g/t → Lowest floatabilities (< 10%) were achieved with PFMAG and PFMQ

Mines	Fe grade (%)	Platy-shaped hematite	Granular Hematite	Martite	Magnetite	Goethite
PFMQ	68.2	0.4	3.4	71.3	4.8	19.2
PFMAG	67.4	0.5	5.0	29,2	58.1	6.6

500g/t → Lowest floatabilities (<10%) were achieved with PFGOE, PXFN, PEAL, PEFN.

Mines	Fe grade (%)	Platy-shaped hematite	Granular Hematite	Martite	Magnetite	Goethite
PEFN	66.9	19.0	60.0	9.3	1.3	9.8
PEAL	68.1	20.5	39.9	25.0	2.3	11.4
PXFN	65.1	11.8	59.7	15.0	4.3	7.6
PFGOE	68.7	0.3	3.3	72.3	1.4	18.8

Depression of Fe-bearing oxides by corn starch
(Flotigam®EDA= 231-462g/t, pH10.5)
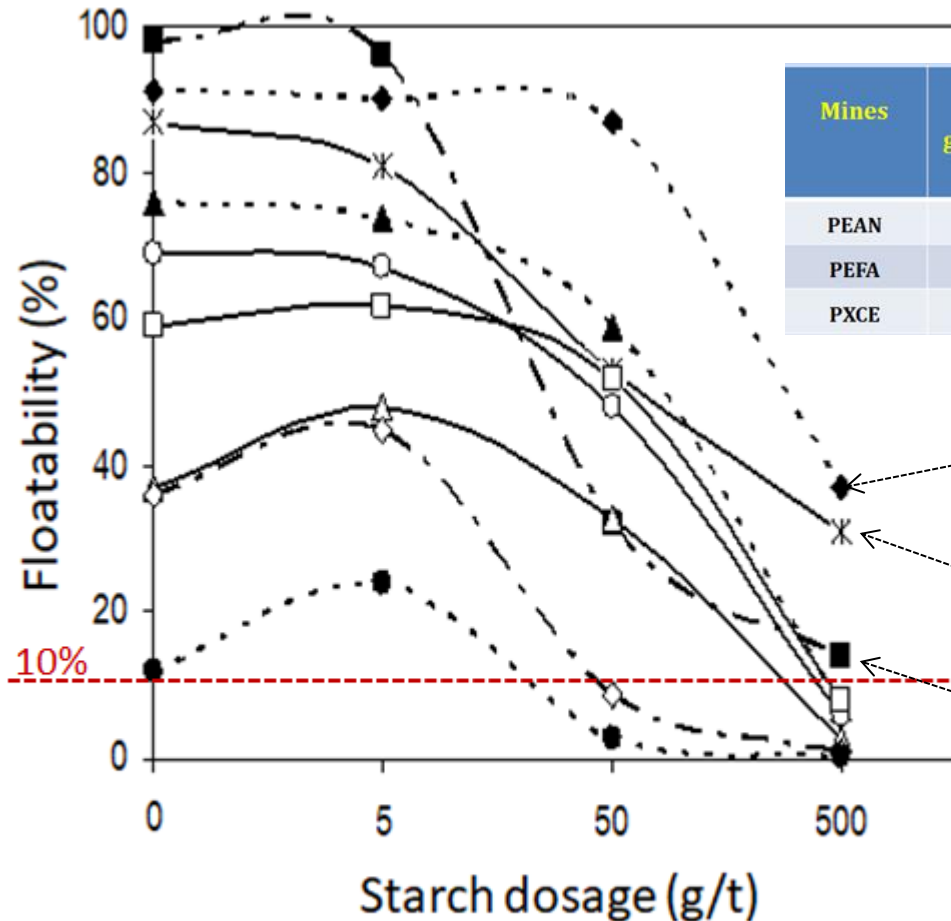
Mines	Fe grade (%)	Platy-shaped hematite	Granular Hematite	Martite	Magnetite	Goethite
PEAN	69.1	24.1	67.2	1.8	0.5	3.4
PEFA	66.6	20.7	66.8	6.3	0.4	4.4
PXCE	68.9	23.7	74.0	0.0	0.1	0.4

The sample PEFA shows the highest content of -37µm (67,1%). Perhaps 500g/t of starch was not sufficient to depress all the Fe-bearing oxides.

PXCE → **98%** of hematite

PEAN → **91%** of hematite

Both samples bear the highest content of platy-shaped hematite (specularite)
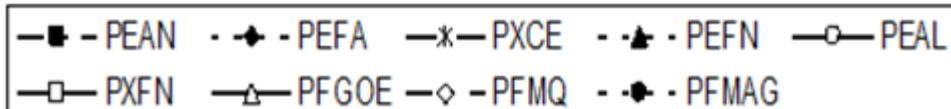
Mine of Brucutu

- 20% of Fe in the flotation tailings in 2015
- A reference in specularite (~38%)

Mines	Content of Fe (%)	Platy-shaped hematite	Granular Hematite	Martite	Magnetite	Goethite
BRUCUTU	68.8	**37.7**	60.3	0,1	0,0	0,1
PEAN	69.1	24,1	67,2	1,8	0,5	3,4
PEFA	66.6	20,7	66,8	6,3	0,4	4,4
PXCE	68.9	23,7	74,0	0,0	0,1	0,4

Starch adsorbs onto hematite particles by surface complexation

Weissenborn et al., 1995   P.K. Weissenborn, L.J. Warren, J.G. Dunn
Selective flocculation of ultrafine iron ore. 1. Mechanism of adsorption of starch onto hematite
Colloids Surf. A: Physicochem. Eng. Aspects, 99 (1995), pp. 11-27

RAJU, B. G.; HOLMGREN, A.; FORSLING, W. (1998) Complexation mechanism of dextrin with metal hydroxides. **J. of Colloid and Interface Science,** 200, pp. 1-6.

RAJU, B. G.; HOLMGREN, A.; FORSLING, W. (1997) Adsorption of dextrin at mineral/water interface. **J. of Colloid and Interface Science,** 193, pp. 215-22.

Surface complexation Model
(Forsling and co-workers)

MINERAL + AMIDO ⇌ MINERAL/AMIDO + ÁGUA

$M = Ca^{2+}$

$M = Fe^{3+}/Fe^{2+}$

$M = Al^{3+}$
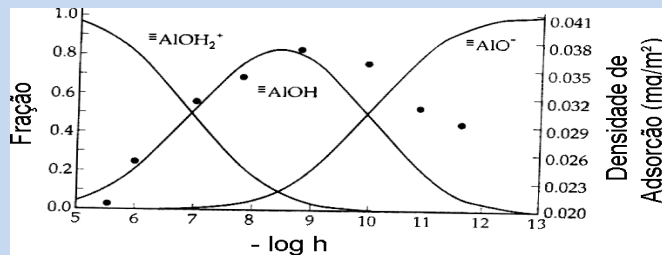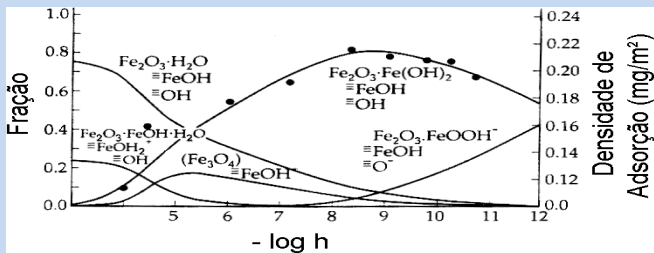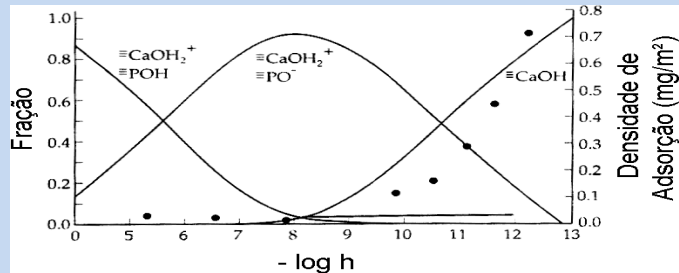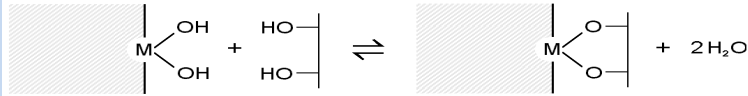
Because calcite and apatite are Ca-bearing minerals, the starch preference towards calcite cannot be fully explained by the model
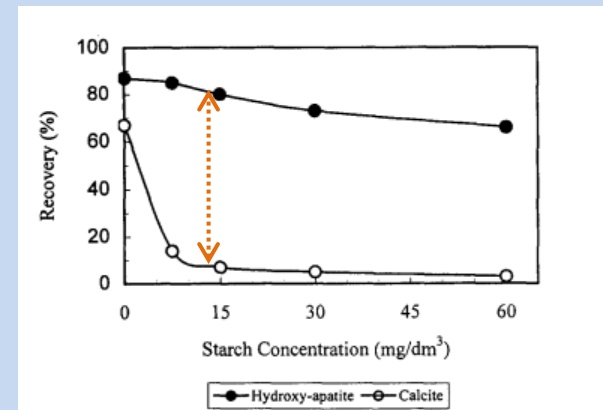
Sodium oleate = 15 mg/L
pH=10.2

Ca-Ca distances (D) on the minerals´ surface may vary according to the crystallographic plane exposed to starch adsorption

Apatite

Calcite

CaOH on **apatite**'s structure – face (001)
CaOH on **apatite**'s structure – face (100)
CaOH on **calcite**'s structure – face (001)
CaOH on **calcite**'s structure – face (021)
CaOH on **calcite**'s structure – face (401)
CaOH on **calcite**'s structure – face (012)
CaOH on **calcite**'s structure – face (211)
CaOH on **calcite**'s structure – face (101)
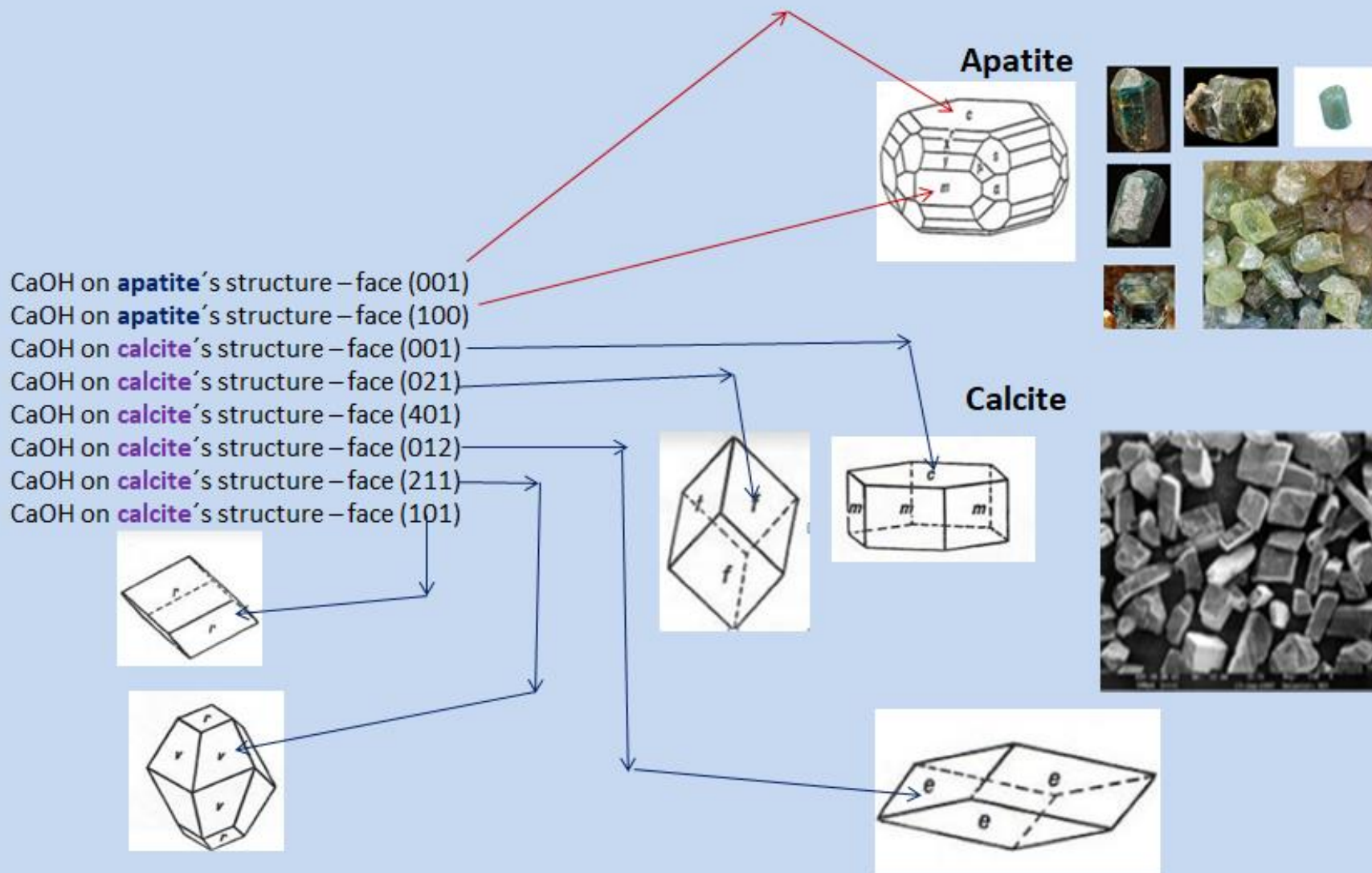
Fitting number model

LEAL FILHO, L.S.; SEIDL, P.R.; CORREIA, J.C.G.; CERQUEIRA, L.C.K. (2000)
Molecular modelling of reagents for flotation processes. **Minerals Engineering**, 13, pp. 1495-1503.

Mineral surface:
Distances (D) between Ca-Ca sites on selected crystallographic planes (hkl)

Structure of the depressant
Distances (d) between OH groups along depressant´s structure

Minerals' structure were constructed by "Crystal Build Module".
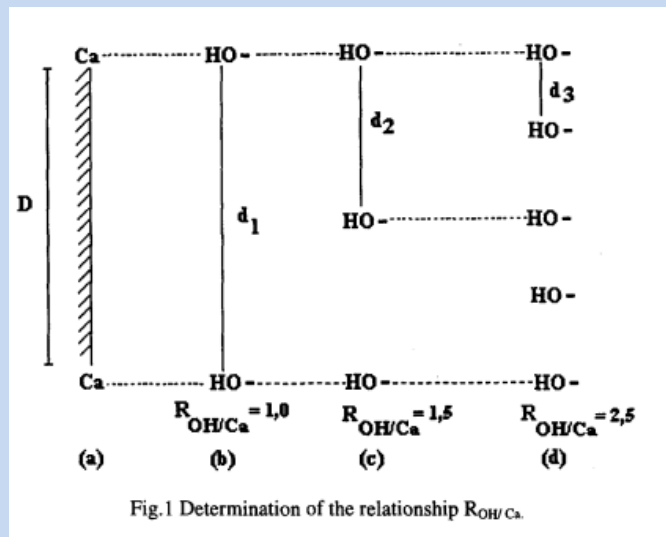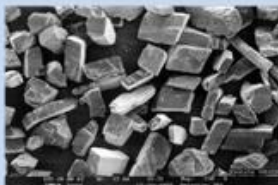
Macromolecules were built by using Polymer builder module (2.0 Cerius environment running on Silicon Graphics 5.1 IRIX operational system). Structures minimized by "Dreiding Force Field".

Fig.1 Determination of the relationship $R_{OH/Ca}$.

$R_{OH/Ca} = 1,0$ (b) $R_{OH/Ca} = 1,5$ (c) $R_{OH/Ca} = 2,5$ (d)
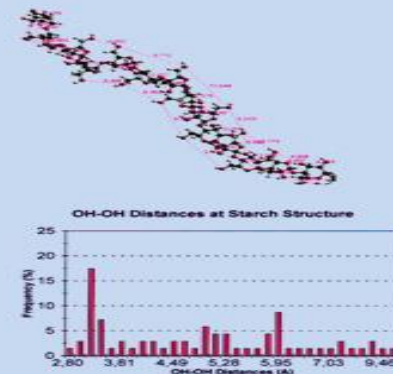
Fitting number model

$$F_{Total} = \sum F_i$$

$$F_i = \sqrt{\frac{F_1 F_2}{R_{OH-Ca}}} = \sqrt{\frac{2F_1 F_2}{(m+1)}}$$

D = m*d   matching number = m   Ratio OH/Ca = $R_{OH/Ca} = \dfrac{m+1}{2}$

"D" on a selected (hkl) plane of the mineral crystal
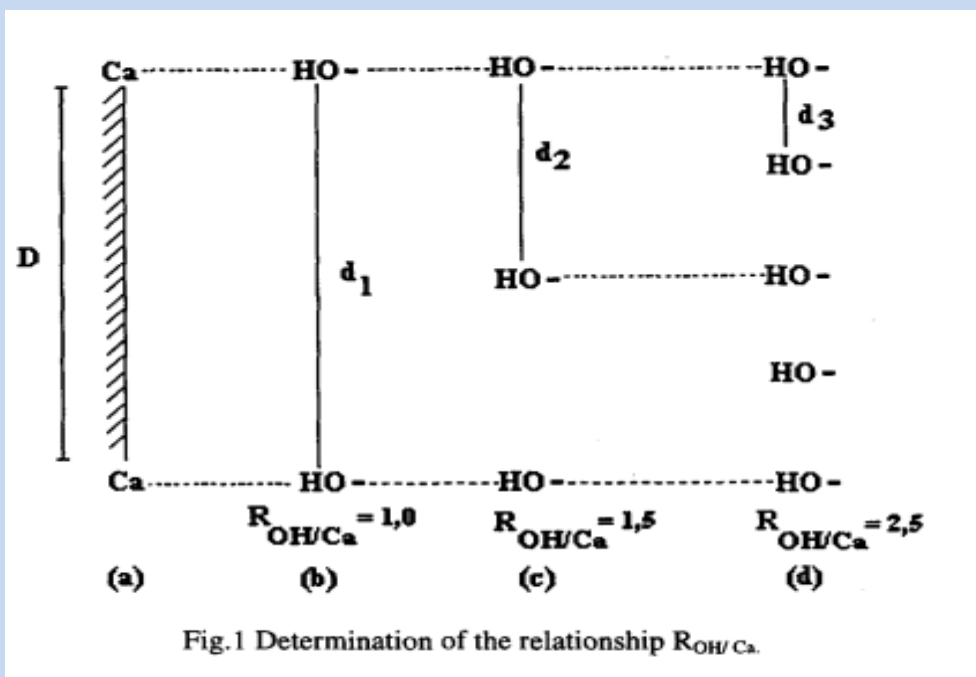
"d" on the polymer's structure

Fig.1 Determination of the relationship $R_{OH/Ca}$.

Fitting number model

$$F_{Total} = \sum F_i$$

$$F_i = \sqrt{\frac{F_1 F_2}{R_{OH-Ca}}} = \sqrt{\frac{2F_1 F_2}{(m+1)}}$$

"D" on a selected (hkl) plane of the mineral crystal

Fig.1 Determination of the relationship $R_{OH/Ca}$.

"d" on the polymer´s structure

D = m * d
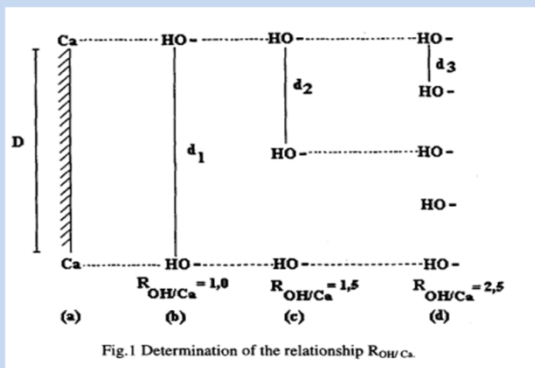
Mineral Ca-Ca (Å)	Polymer OH-OH (Å)	matching number (m)
4.99	4.99	1
6.36	6.36	1
9.50	3.18	3
9.97	4.99	2
12.72	3.18	4
13.77	6.88	2
14.96	4.99	3
17.73	2.95	6
18.41	6.15	3
19.09	3.18	6
19.94	4.99	4
23.41	4.68	5
25.45	3.18	8
27.54	6.88	4
30.75	6.15	5

Calcite (101)

"D" on a selected (hkl) plane of the mineral crystal

Fig.1 Determination of the relationship $R_{OH/Ca}$.

"d" on the polymer´s structure

D = m * d
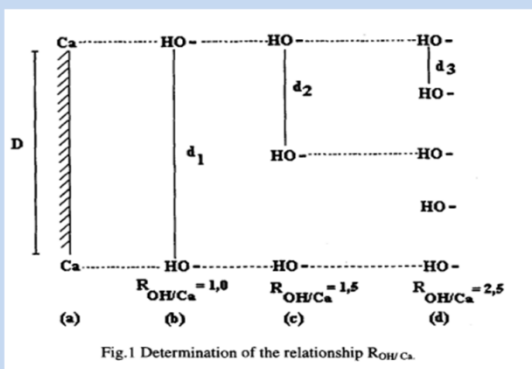
Mineral Ca-Ca (Å)	Polymer OH-OH (Å)	matching number (m)
5.43	5.40	1
10.87	3.63	3
19.59	2.80	7
23.68	3.95	6

Apatite (001)

Fitting number model

$$F_i = \sqrt{\frac{F_1 F_2}{R_{OH-Ca}}} = \sqrt{\frac{2F_1 F_2}{(m+1)}}$$

$F_{Total} \rightarrow$ varies between 0 and 100

Starch-calcite (101)

| d Ca-Ca	F1	m	d OH-OH	m x dOH-OH	F2	Δ	K	SQRT (K)
4,99	2,5	1	4,99	4,99	5,80	0,00	14,50	3,81
6,36	5,0	2	3,18	6,36	17,39	0,00	57,97	7,61
9,50	5,0	3	3,18	9,54	17,39	-0,04	43,48	6,59
9,97	2,5	2	4,99	9,98	5,80	-0,01	9,67	3,11
11,71	2,5	0	0,00	0,00	0,00	11,71	0,00	0,00
12,72	5,0	4	3,18	12,72	17,39	0,00	34,78	5,90
13,77	5,0	2	6,88	13,76	1,45	0,01	4,83	2,20
14,96	2,5	3	4,99	14,97	5,80	-0,01	7,25	2,69
15,37	5,0	0	0,00	0,00	0,00	15,37	0,00	0,00
17,73	5,0	6	2,95	17,70	2,90	0,03	4,14	2,04
18,41	5,0	3	6,15	18,45	1,45	-0,04	3,63	1,90
18,99	5,0	0	0,00	0,00	0,00	18,99	0,00	0,00
19,09	5,0	6	3,18	19,08	17,39	0,01	24,84	4,98
19,94	2,5	4	4,99	19,96	5,80	-0,02	5,80	2,41
21,53	5,0	0	0,00	0,00	0,00	21,53	0,00	0,00
23,12	2,5	0	0,00	0,00	0,00	23,12	0,00	0,00
23,18	2,5	0	0,00	0,00	0,00	23,18	0,00	0,00
23,41	2,5	5	4,68	23,40	2,90	0,01	2,42	1,55
23,94	5,0	0	0,00	0,00	0,00	23,94	0,00	0,00
24,76	2,5	0	0,00	0,00	0,00	24,76	0,00	0,00
25,45	5,0	8	3,18	25,44	17,39	0,01	19,32	4,40
27,54	2,5	4	6,88	27,52	1,45	0,02	1,45	1,20
27,78	2,5	0	0,00	0,00	0,00	27,78	0,00	0,00
28,49	2,5	0	0,00	0,00	0,00	28,49	0,00	0,00
30,75	2,5	5	6,15	30,75	1,45	0,00	1,21	1,10
32,56	2,5	0	0,00	0,00	0,00	32,56	0,00	0,00
34,20	2,5	0	0,00	0,00	0,00	34,20	0,00	0,00
37,99	2,5	0	0,00	0,00	0,00	37,99	0,00	0,00
							Ft =	51,50

$$\sqrt{\frac{2*2.5*5.0}{(1+1)}} = 3.81$$

$$D = d*m$$

$$\sqrt{\frac{2*5.0*17.39}{(2+1)}} = 7.61$$

$$\sqrt{\frac{2*2.5*2.90}{(5+1)}} = 1.55$$

$$F_{Total} = \sum F_i = 51.5$$

Fitting number model

$$F_i = \sqrt{\frac{F_1 F_2}{R_{OH-Ca}}} = \sqrt{\frac{2F_1 F_2}{(m+1)}}$$

$F_{Total} \rightarrow$ varies between 0 and 100

Starch-Apatite (001)

d Ca–Ca	F1	m	D OH–OH	m x dOH–OH	F2	B–F	K(*)	SQRT (K)
5.43	6.12	1	5.40	5.40	1.45	0.03	8.87	2.98
9.41	12.24	0	0.00	0.00	0.00	9.41	0.00	0.00
10.87	6.12	3	3.63	10.89	1.45	-0.02	4.44	2.11
14.37	8.16	0	0.00	0.00	0.00	14.37	0.00	0.00
14.38	4.08	0	0.00	0.00	0.00	14.38	0.00	0.00
16.30	12.24	0	0.00	0.00	0.00	16.30	0.00	0.00
18.82	12.24	0	0.00	0.00	0.00	18.82	0.00	0.00
19.59	12.24	7	2.80	19.60	1.45	-0.01	4.44	2.11
21.73	2.04	0	0.00	0.00	0.00	21.73	0.00	0.00
23.68	4.08	6	3.95	23.70	1.45	-0.02	1.69	1.30
24.90	8.16	0	0.00	0.00	0.00	24.90	0.00	0.00
27.16	2.04	0	0.00	0.00	0.00	27.16	0.00	0.00
30.25	4.08	0	0.00	0.00	0.00	30.25	0.00	0.00
32.60	4.08	0	0.00	0.00	0.00	32.60	0.00	0.00
38.03	2.04	0	0.00	0.00	0.00	38.03	0.00	0.00
							TOTAL =	**8.49**

$$\sqrt{\frac{2*6.12*1.45}{(1+1)}} = 2.98$$

$$\sqrt{\frac{2*6.12*1.45}{(3+1)}} = 2.11$$

$$\sqrt{\frac{2*12.24*1.45}{(7+1)}} = 2.11$$

$$\sqrt{\frac{2*4.08*1.45}{(6+1)}} = 1.30$$

D= d*m

Mineral	Polymer	matching
Ca-Ca	OH-OH	number
(Å)	(Å)	(m)
5.43	5.40	1
10.87	3.63	3
19.59	2.80	7
23.68	3.95	6

$$F_{Total} = \sum F_i = 8.5$$

Values of Ft for apatite and calcite

Polímeros → Minerais (hkl) ↓	Starch	Tanino L-36	Goma Guar	Etil Celulose
Apatita (001)	8,5	11,2	12,6	14,9
Apatita (010)	25,7	26,5	17,2	23,6
Calcita (101)	51,5	37,6	11,0	13,7
Calcita (021)	30,2	23,1	2,4	4,7
Calcita (401)	20,1	33,4	0,0	12,2
Calcita (012)	39,1	27,8	7,5	17, 3
Calcita (001)	43,7	38,4	0,0	17,5
Calcita (211)	36,8	13,9	3,3	18,1

The model indicates that starch adsorbs preferentially onto calcite´s surface instead of apatite´s surface.

4. Handling of pellet feed

4.1 Critical velocity for coarse particle settling in pressurized pipes;

4.2 Wind drag simulation of pellet feed during railway transportation;

4.3 Fast elimination of moisture from iron ore concentrates by blowing heat and dry air.

From its origin (mine/mineral processing plant) to the ports, hematite concentrates must be conveyed by large distances (500-900km).

1. Railway from Carajás-PA to São Luís-MA
2. Railway from Minas Gerais to Vitória-ES
3. Railway from Minas Gerais to Itaguaí-RJ
4. Waterway from Mato Grosso to Buenos Aires (Argentina)

There is much concern on:

(a) the environmental impact of railway transportation of concentrates on neighboring communities;

(b) How to carry out hydraulic convey of sinter feed without previous grinding (-74μm)?

Modelling the critical velocity (V_C) for coarse particles settling into pipelines

Fig. 1. Schematic of recirculating pipeline test rig.
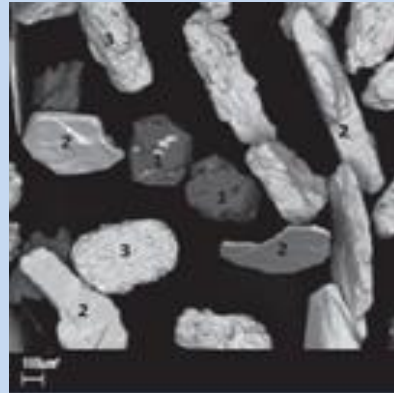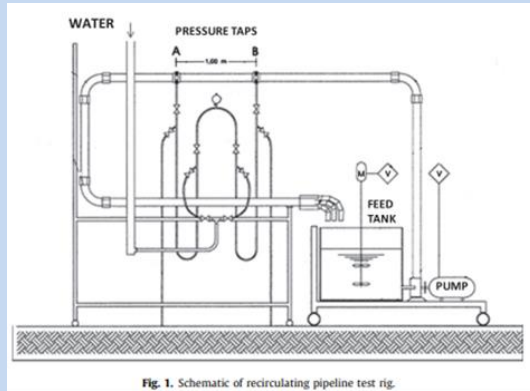
1. Quartz
2. Platy shaped hematite
3. Granular (rounded) hematite

Sphericity function (Ψ) is an assessment of how closely a particle approaches a spherical configuration.

It is the ratio of the surface of a sphere (s) which has the same volume as a particle which exhibits surface area S.

$$\Psi = \frac{s}{S}$$
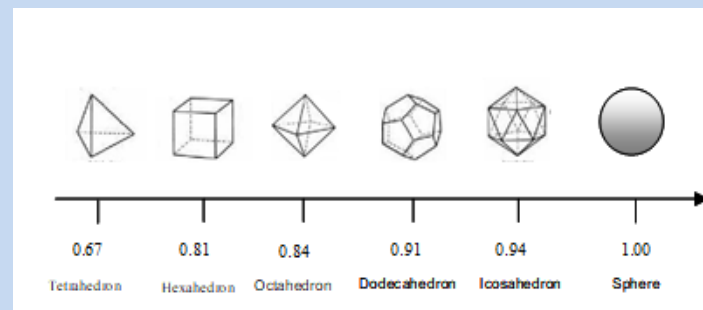
Determined by the percolation of gas through packed beds

| 0.67 | 0.81 | 0.84 | 0.91 | 0.94 | 1.00 |
| Tetrahedron | Hexahedron | Octahedron | Dodecahedron | Icosahedron | Sphere |

Although a population of hematite particles show an overall value of sphericity function (Ψ = 0.38), the rounded particles (0.50 < Ψ < 0.58) behaved in a different way than platy-shaped particles (0.27 < Ψ < 0.33)

Table 2
Information on mineral samples used in the model.

Sample	Sauter mean diameter (μm)		Specific gravity	Sphericity function (Ψ)	
	Class-1	Class-2		Class-1	Class-2
Quartz	265	132	2.620	0.80	0.81
Apatite	295	151	3.130	0.63	0.64
Hematite	336	163	4.900	0.39	0.37
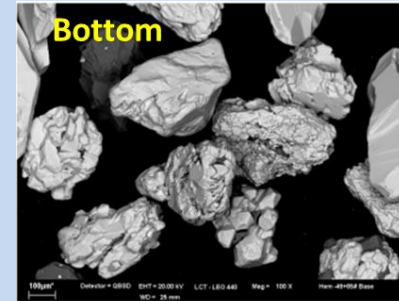
Fig. 8. Hematite particles from the bottom of the pipe (gutter section 3).
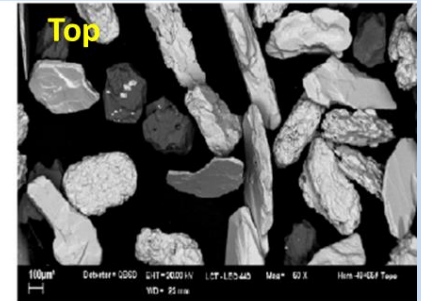
Fig. 10. Hematite particles from the top of the pipe (gutter section 1).

$$V_c = 0.124(S_s - 1)^{0.5}\left(\frac{d_s \cdot \rho_m \cdot \sqrt{g \cdot D}}{\mu_f}\right)^{0.37} \cdot \left(\frac{d_s \cdot \Psi}{D}\right)^{-0.007} e^{3.10 \cdot C_v}$$
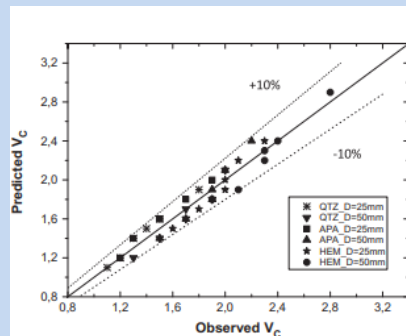
Fig. 11. Observed versus predicted critical velocity, m/s.
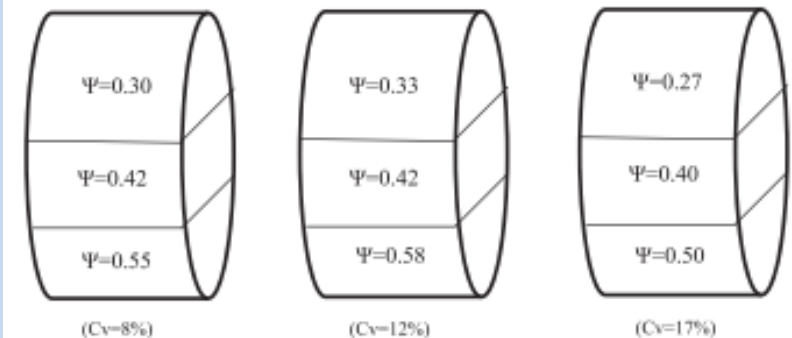
Fig. 7. Sphericity function according to the gutter pipe section for hematite concentrate (0.105 mm < d < 0.149 mm).

Why Fe-concentrates (pellet feed) from different mines emit dust in different amounts during the conveying by railway?

1. Fábrica Nova (PXFN)
2. Brucutu (PXBR)
3. Conceição/Cauê (PXCE)

Wind drag simulation of sinter feed during railway transportation

- Content of fines (-37μm)
- Ore moisture (%)
- Sphericity
- Wind speed
- Temperature
- Air moisture
- Mineralogy

Loss of mass during the experiments (%P)

$$\%P = 100 \left(\frac{M_i - M_f}{M_i} \right)$$
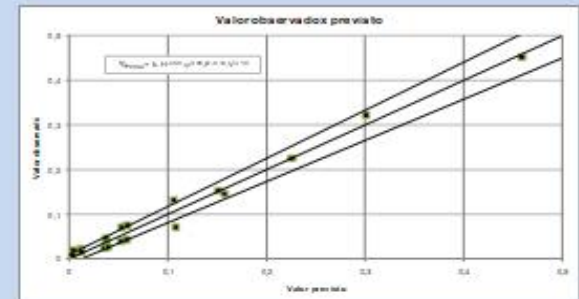
$$\%P = K \cdot H^{-4,58} \cdot \Psi^{9,84} \cdot F^{-0,13} \cdot V^{3,18}$$

K = Constant
H = Ore´s moisture content
Ψ = Sphericity
F = Content of fines
V = Wind velocity

The model gave subsides for dust control along the railway

"Samarco Award" – ABM (Brazilian Association for Metallurgy, Materials and Mining)

The model was enhanced by approaching new variables (U,T) and considering ore piles

$$\%P = K \cdot H^{-4.37} \Psi^{-18.59} F^{7.88} V^{3.78} U^{-2.63} T^{1.88}$$

K = Empirical constant: $\left(\frac{s}{m}\right)^{3.78} {}^o C^{-1.88}$

H = Ore´s moisture content (%);

Ψ = Sphericity function;

F = Content of fines (%)

V= Wind velocity (m/s)

U = Relative moisture in the air (%)

T = Air temperature (ᵒC) (dry bulb)

Dust

13-25 g$_{H2O}$ per kg of air

12.5% of moisture
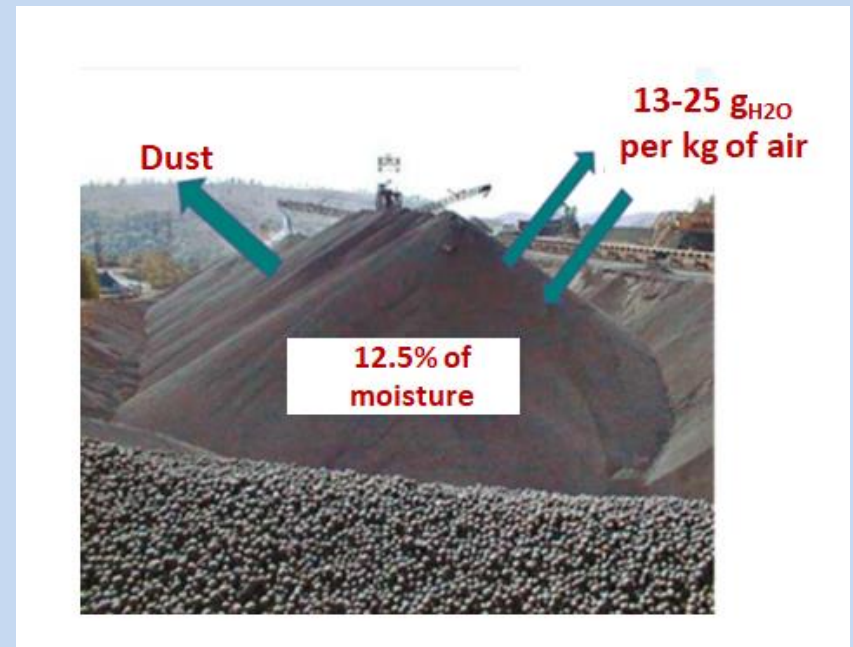
Decrease in iron ore moisture content to achieve the limits posed by the International Maritime Organization (IMO)

TML = "Tolerable Moisture Limit"

The highest moisture content an ore can exhibit to embark on a ship to avoid accidents.

Concentrates are unloaded from the railway wagons and spend up to 5 days in the yard of the ports before shipping.

PÓ

AR (H_2O)

ÁGUA

MINÉRIO (H_2O)
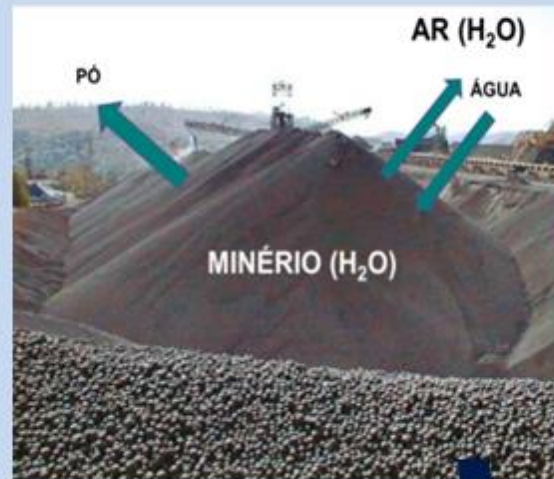
Concentrates are ready for shipping if they bear a moisture content $\leq$ TML

$$\%P = K \cdot H^{-4.37} \Psi^{-18.59} F^{7.88} V^{3.78} U^{-2.63} T^{1.88}$$

Dust

13-25 g_{H2O} per kg of air
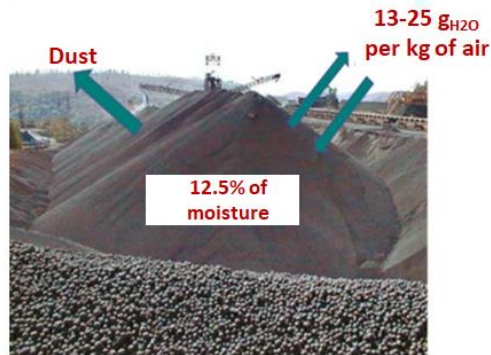
12.5% of moisture

Moisture content in the air played a more significant role in dust generation (a result from water evaporation)
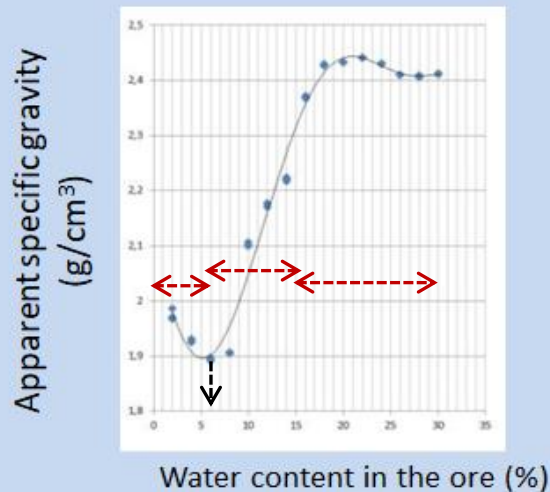
6% of moisture is a critical value

Apparent specific gravity (g/cm³)

Water content in the ore (%)

Moisture range (%)	Nature of the water	Process to remove water
0-6	Adsorbed water	Drying
6-15	Capillary water	Filtering aids
>15	Free water	Spontaneous flow
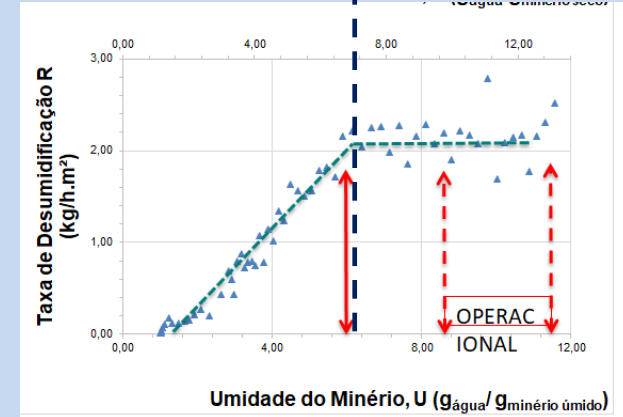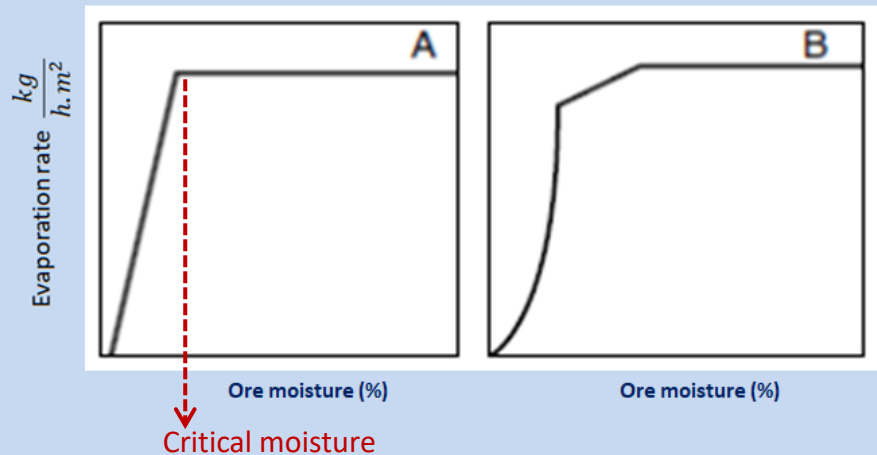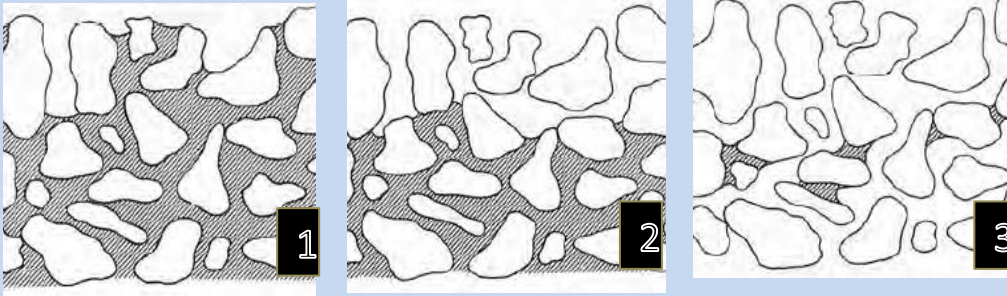
The experiments indicated the need of blowing dry air (3-5 g of water per kg of air) against the ore flow in conveyor belts or transference chutes.

The destruction of the capillaries partially filled by water could enhance the decrease of moisture in the pellet feed

Moisture in the feed (%)	Where to blow dry air?	Moisture in the product	Moisture reduction (%)	Cost assessment	
				Electricity U$/ton	Burning of gas U$/ton
11.8 ± 0.1	Conveyor belt	10.0 ± 0.1	1.8	2,40	1,18
12.2 ± 0.2	Transference Chute	10.4 ± 0.2		0,19	0,03
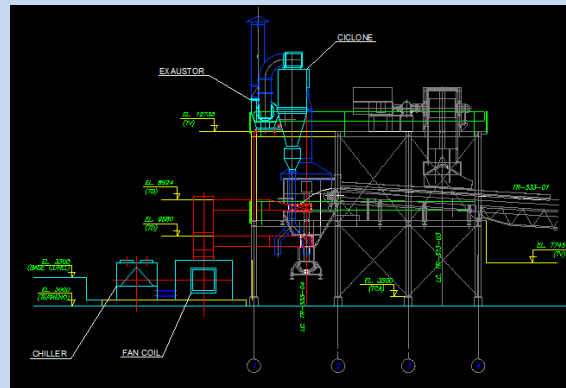
Granted charters around the world
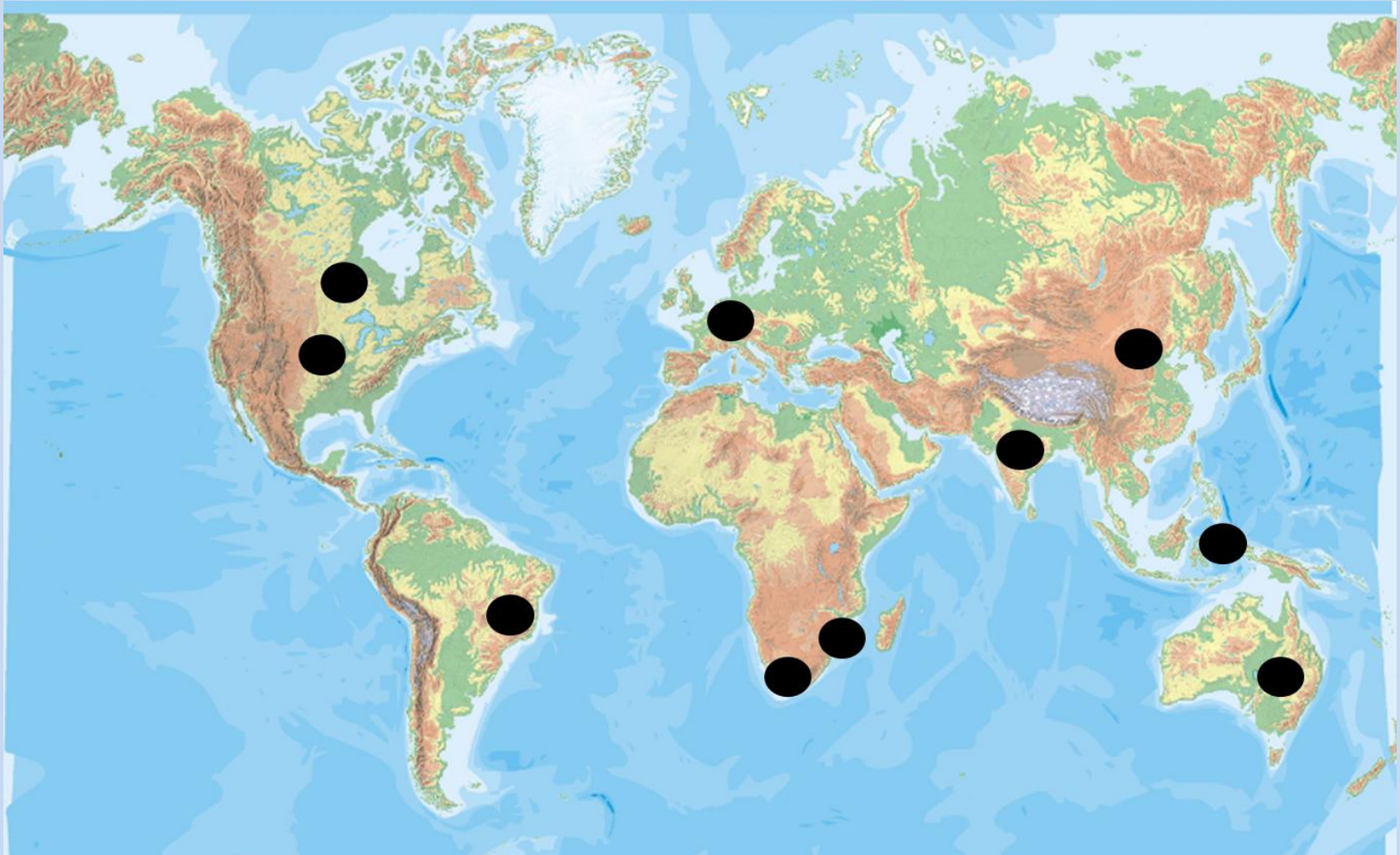
6. Concluding remarks

Concluding Remarks

1) **Reverse cationic flotation of quartz from standard itabirite has been conducted for more than 40 years:**

- Desliming before flotation is mandatory to avoid excessive frothing;

- Cationic reverse flotation of quartz is carried out in basic medium (9.0 < pH < 10.5), using starch (corn or manioc) as depressant for Fe-bearing oxides and alkyl (C_{10}) ether amine as collector.

-Traditional reagent scheme fails to concentrate dolomitic and amphibolitic itabirite;

- Water quality is an issue, mostly when contaminated by Ca^{2+}, Mg^{2+} and Mn^{2+} ;

Concluding Remarks

2) High contents of SiO_2 in the final concentrate jeopardize the quality of sinter feed. This problem happens because:

-Poor flotation of coarse particles of quartz (+0,10mm) at reverse cationic flotation is a problem. Higher contact angles and/or enhanced equipment (that produce less turbulence) are required do improve the rejection of quartz;

- Because the detachment of particles from bubbles are likely to occur in either mechanical or column cells, the bad reputation of the latter to float coarse particles seems to be related to the fact that mechanical cells are mixers whereas columns are plug flow reactors. This way, due to the higher internal slurry recirculation offered by mechanical cells, detached hydrophobic coarse particles will have more opportunities to collide with bubbles and float.

Concluding Remarks

3) About the depression of Fe-bearing oxides with corn starch:

- Corn starch is prepared by leaching with NaOH (gelatinization) and the best mass ratio of starch/NaOH lay in the range: from 4.5:1 up to 5:1;

- It is not mandatory to use purified starch (white flour). The yellow flour (gritz) is 3 times cheaper and also very effective;

-Corn starch depresses magnetite, martite and goethite very well at low dosages (50g/t), but it fails to depress 100% of hematite even at a dosage of 500g/t when hematite shows high amount of platy-shaped particles (as it occurs in Brucutu mine). The use of tannins could improve the depression of hematite.

Concluding Remarks

4) Regarding the handling of pellet feed

- Pellet feed yielded from iron ore in which hematite particles show platy-shaped habitus (mostly specularite) exhibit greater propensity to be levitated and spread by the air;

- In pipelines, platy-shaped particles tend to concentrate in the top of the pipe, whereas rounded (granulate) particles in the bottom;

- To meet the specifications posed by the International Maritime Organization (IMO), concentrates must show moisture degree lower than the TML (Tolerable Moisture Level). In the yards of the ports, to make fast and small corrections in ore moisture before loading the ships, a process based on blowing dry and heat air was developed by Vale Institute of Technology (ITV).

References

- GAUDIN, A.M.; FUERSTENAU, D.W. (1955) Quartz flotation with cationic collectors. *Trans. AIME*, 202, pp. 958-962.

- SMITH, R.W.; SCOTT, J.L. (1990) Mechanisms of dodecyl amine flotation of quartz. *Mineral Process. Ext. Metall*, 7, pp. 81-94.

- LASKOWSKI, VURDELA, LIU (1988) The colloid chemistry of weak electrolyte collector flotation. In: FORSBERG, E.K.S., *Proceedings of 16th International Mineral Processing Congress – Developments in Mineral Processing*, Elsevier, pp.703-715.

- VIDYADHAR, A.; RAO, H.K.; CHERNYSHOVA, I.V.; PRADIP,K.S.; FORSBERG, E. (2002) Mechanisms of amine-quartz interaction in the absence and presence of alcohols studied by spectroscopic methods. *J. of colloid and interface science*, 256, pp. 59-72.

- WHISTLER, R.L.; PASCHALL, E.F. (1965). *Starch: Chemistry and Technology*, vol. 1, Academic Press, New York.

- PINTO, C.L.L.; ARAUJO, A.C.; PERES, A.E.C. (1992) The effect of starch, amylose and amylopectin on the depression of oxi-minerals. *Minerals Engineering*, 5, pp. 469-78.

- LEAL FILHO, L.S.; SEIDL, P.R.; CORREIA, J.C.G.; CERQUEIRA, L.C.K. (2000) Molecular modelling of reagents for flotation processes. *Minerals Engineering*, 13, pp. 1495-1503.

- BALAJEE, S.R.; IWASAKI, I. (1969) Adsorption mechanisms of starches in flotation and flocculation of iron ores. Trans. AIME, vo. 244, pp. 401-406.

- GONTIJO, C.F. (2010) Adsorção de amina em quartzo para flotação reversa de minério de ferro. Anais do *41⁰. Seminário de redução de minério de Ferro e 12⁰. Simpósio de Minério de Ferro*, ABM, Belo Horizonte.

- RALSTON, J. FORNASIERO, D.; HAYES, R. (1999) Bubble-particle attachment and detachment in flotation. International Journal of Mineral Processing, 56, pp.133-164.

www.ibram.org.br

www.inthemine.com.br/site/estrutura-produtiva-do-minerio-de-ferro-no-brasil

References

- KRAMER, A.; GAULOCHER, S.; MARTINS, M.;LEAL FILHO, L.S. (2012) Surface Tension Measurement for Optimization of Flotation Control. *Procedia Engineering*, 46, pp. 111-118.

- SCHULZE, H. J. (1984*) Physicochemical elementary processes in flotation*. Elsevier, Amsterdam, p. 348.

- SOUZA PINTO, T.C.; LIMA, O.A.; LEAL FILHO, L.S. (2009) Sphericity of apatite particles determined by gas permeability through packed beds. *Minerals & Metallurgical Processing*, 26, pp. 105-108.

- LEAL FILHO, L.S.; SEIDL, P.R.; CORREIA, J.C.G. (1998*) Estudos de Modelagem Molecular Visando à Otimização da Depressão de Hematita - Contrato CVRD T-0071/97*. Escola Politécnica da Universidade de São Paulo, São Paulo, 49p.

- MARTINS, M.; LIMA, N.P.; LEAL FILHO, L.S. (2012) Depressão de minerais de ferro: influência da mineralogia, morfologia e pH de condicionamento. *Revista da Escola de Minas*, 65, pp. 393-399.

- LEAL FILHO, L.S.; SEIDL, P.R.; CORREIA, J.C.G.; CERQUEIRA, L.C.K. (2000) Molecular modelling of reagents for flotation processes. *Minerals Engineering*, 13, pp. 1495-1503.

- SOUZA PINTO, T.C.; COSTA, M.A.; SILVA, D.F.S.; LEAL FILHO, L.S. (2020) Process for ore moisture reduction in conveyor belts and transfer chutes. European Patent Office 3368849. Date of the application: 10/27/2015. Date of grant of the charter: 12/23/2020. Patent ownership: Vale S.A.

- SAFARI, M.; HOSEINIAN, F.S.; DEGLON, D.A.; LEAL FILHO, L.S.; SOUZA PINTO, T.C. (2022) Impact of flotation operational parameters on the optimization of fine and coarse Itabirite iron ore beneficiation. *Powder Technology*, 408, p.117772.

- FELIX, L.L.; MOREIRA, G.F.; LEAL FILHO, L.S.; STAVALE, F. (2022) Starch adsorption on hematite surfaces: evidence of the adsorption mechanism dependence on the surface orientation. *Minerals Engineering,* 178, pp. 107429.

TOHRY, A.; DEHGHAN, R.; LEAL FILHO, L.S.; CHELGANI, S.C. (2021) Tannin: An eco-friendly depressant for the green flotation separation of hematite from quartz. *Minerals Engineering*, 168, p. 106917.

References

- SILVA, K.; FILLIPOV, L.O.; PIÇARRA, A.; FILLIPOVA, I.V.; FAUSTINO, L.M.; SKLIAR, A.; LIMA, N.; LEAL FILHO, L.S. (2021) New perspectives in iron ore flotation: Use of collector reagents without depressants in reverse cationic flotation of quartz. *Minerals Engineering*, 170, p. 107004.

- GELDENHUYS, S.; SOUZA PINTO, T.C.; LEAL FILHO, L.S.; DEGLON, D.A. (2021) Process Evaluation of an Iron Ore Operation Using the Floatability Component Model. *Minerals*, 11, p. 589.

- CALDERÓN-HERNANDEZ, J. W.; SINATORA, A.; MELO, H.G.; CHAVES, A.P.; MANO, E.S.; LEAL FILHO, L.S.; PAIVA, J.L.; BRAGA, A.S.; SOUZA PINTO, T.C. (2020) Hydraulic convey of iron ore slurry: pipeline wear and particle degradation in function of pumping time. *Wear*, 450-451, p. 203272.

- ROHEM, E.P.; ALBUQUERQUE, M.D.F.; ANTOUN, R.S.; LEAL FILHO, L.S.; MONTE, M.B.M. (2019) Interaction forces between colloidal starch, quartz and hematite particles. *Colloids and Surfaces A – Physicochemical and Engineering Aspects*, vol. 562, pp. 79-85.

- NYKANEN, V.P.S; BRAGA, A.S.; SOUZA PINTO, T.C.; MATAI, P.H.L.S.; LIMA, N.P.; LEAL FILHO, L.S.; Monte, M.B.M. (2018) True Flotation versus Entrainment in Reverse Cationic Flotation for the Concentration of Iron Ore at Industrial Scale. *Mineral Processing and Extractive Metallurgy Review* (ISSN 1061-2971).

- MOREIRA, G.F.; PEÇANHA, E.R.; MONTE, M.B.M.; Leal Filho, L.S.; STAVALE, F. (2017) XPS study on the mechanism starch-hematite surface chemical complexation. *Minerals Engineering* (ISSN 0892-6875), vol. 110, pp. 96-103.

- SOUZA PINTO, T.C.; SLATTER, P.T.; MATAI, P.H.L.S.; LEAL FILHO, L.S. (2016). The influence of hematite particle shape on stratification in pipe flow. *Powder Technology* (ISSN 0032-5910), vol. 302, pp. 75-80.

- SOUZA PINTO, T.C.; MORAES JÚNIOR, D.; SLATTER, P.T.; LEAL FILHO, L.S.(2014). Modelling the critical velocity for heterogeneous flow of mineral slurries. *International Journal of Multiphase Flow* (ISSN 0301-9322), vol. 65, pp. 31-37.
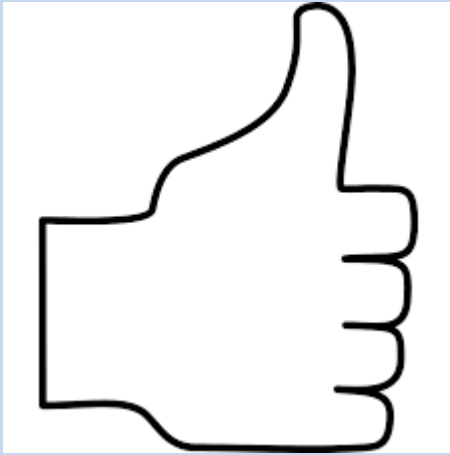
Obrigado

Laurindo de S. Leal Filho

lauleal@usp.br
+5511 999 81 10 37